









Evolutionary and Phenotypic Characterization of Two Spike Mutations in European Lineage 20E of SARS-CoV-2

 Paula Ruiz-Rodríguez,^a  Clara Francés-Gómez,^a Álvaro Chiner-Oms,^b Mariana G. López,^b Santiago Jiménez-Serrano,^b Irving Cancino-Muñoz,^b Paula Ruiz-Hueso,^c Manuela Torres-Puente,^b María Alma Bracho,^{a,d} Giuseppe D'Auria,^{a,c,d} Lúcia Martínez-Priego,^c Manuel Guerreiro,^{e,f} Marta Montero-Alonso,^g María Dolores Gómez,^h José Luis Piñana,ⁱ SeqCOVID-SPAIN Consortium, Fernando González-Candelas,^{a,d}  Iñaki Comas,^{b,d}  Alberto Marina,^{b,j}  Ron Geller,^a  Mireia Coscolla^a

^a¹SysBio, University of Valencia-CSIC, FISABIO Joint Research Unit Infection and Public Health, Valencia, Spain

^bInstituto de Biomedicina de Valencia, Consejo Superior de Investigaciones Científicas, Valencia, Spain

^cSequencing and Bioinformatics Service of Valencian Region Foundation for the Promotion of Health and Biomedical Research, Valencia, Spain

^dCIBER in Epidemiology and Public Health, Madrid, Spain

^eHematology Department, Hospital Universitari i Politècnic La Fe, Valencia, Spain

^fInstituto de Investigación Sanitaria La Fe, Valencia, Spain

^gInfectious Diseases Unit, Hospital Universitari i Politècnic La Fe, Valencia, Spain

^hMicrobiology Department, Hospital Universitari i Politècnic La Fe, Valencia, Spain

ⁱHematology Service, Hospital Clínico Universitario, Institute for Research INCLIVA, Valencia, Spain

^jCIBER in Rare Diseases, Madrid, Spain

Paula Ruiz-Rodríguez and Clara Francés-Gómez contributed equally to this work. Author order was determined by contribution to the integration of results and writing the manuscript.

ABSTRACT We have detected two mutations in the spike protein of severe acute respiratory syndrome coronavirus 2 (SARS-CoV-2) at amino acid positions 1163 and 1167 that appeared independently in multiple transmission clusters and different genetic backgrounds. Furthermore, both mutations appeared together in a cluster of 1,627 sequences belonging to clade 20E. This cluster is characterized by 12 additional single nucleotide polymorphisms but no deletions. The available structural information on the S protein in the pre- and postfusion conformations predicts that both mutations confer rigidity, which could potentially decrease viral fitness. Accordingly, we observed reduced infectivity of this spike genotype relative to the ancestral 20E sequence *in vitro*, and the levels of viral RNA in nasopharyngeal swabs were not significantly higher. Furthermore, the mutations did not impact thermal stability or antibody neutralization by sera from vaccinated individuals but moderately reduce neutralization by convalescent-phase sera from the early stages of the pandemic. Despite multiple successful appearances of the two spike mutations during the first year of SARS-CoV-2 evolution, the genotype with both mutations was displaced upon the expansion of the 20I (Alpha) variant. The midterm fate of the genotype investigated was consistent with the lack of advantage observed in the clinical and experimental data.

IMPORTANCE We observed repeated, independent emergence of mutations in the SARS-CoV-2 spike involving amino acids 1163 and 1167, within the HR2 functional motif. Conclusions derived from evolutionary and genomic diversity analysis suggest that the co-occurrence of both mutations might pose an advantage for the virus and therefore a threat to effective control of the epidemic. However, biological characterization, including *in vitro* experiments and analysis of clinical data, indicated no clear benefit in terms of stability or infectivity. In agreement with this, continuous epidemiological surveillance conducted months after the first observations revealed that both mutations did not successfully outcompete other variants and stopped circulating 9 months after their initial detection. Additionally, we evaluated the potential of both

Citation Ruiz-Rodríguez P, Francés-Gómez C, Chiner-Oms Á, López MG, Jiménez-Serrano S, Cancino-Muñoz I, Ruiz-Hueso P, Torres-Puente M, Bracho MA, D'Auria G, Martínez-Priego L, Guerreiro M, Montero-Alonso M, Gómez MD, Piñana JL, SeqCOVID-SPAIN Consortium, González-Candelas F, Comas I, Marina A, Geller R, Coscolla M. 2021. Evolutionary and phenotypic characterization of two spike mutations in European lineage 20E of SARS-CoV-2. *mBio* 12:e02315-21. <https://doi.org/10.1128/mBio.02315-21>.

Editor Carmen Buchrieser, Institut Pasteur

Copyright © 2021 Ruiz-Rodríguez et al. This is an open-access article distributed under the terms of the [Creative Commons Attribution 4.0 International license](https://creativecommons.org/licenses/by/4.0/).

Address correspondence to Ron Geller, ron.geller@uv.es, or Mireia Coscolla, mireia.coscolla@uv.es.

Received 11 August 2021

Accepted 8 October 2021

Published 16 November 2021

mutations to escape neutralizing antibodies, finding that the presence of these two mutations on their own is not likely to confer antibody escape. Our results provide an example of how newly emerged spike mutations can be assessed to better understand the risk posed by new variants and indicate that some spike mutations confer no clear advantage to the virus despite independently emerging multiple times and are eventually displaced by fitter variants.

KEYWORDS SARS-CoV-2, spike, HR2, variants, homoplasy, antibody escape, adaptive mutations

Genomic surveillance of viral mutations is the first step in detecting viral changes that could impact public health by interfering with diagnostics, modifying pathogenicity, or altering susceptibility to existing immunity or treatments. In many countries, the challenge of detecting new mutations of interest in severe acute respiratory syndrome coronavirus 2 (SARS-CoV-2) involves sequencing representative genomes from circulating viruses, sharing sequence information on public databases (e.g., GISAID [1]), and analyzing them in real time using platforms such as Nextstrain (2). While mutations appear randomly, their fate in the population depends on a combination of the conferred fitness advantage and stochastic and demographic processes. A first step in assessing the potential public health impact of newly observed mutations is to determine whether their increase in frequency is due to chance or adaptation. If they are found to be adaptive, it is important to evaluate whether their adaptation is linked to an improved ability to replicate, colonize, transmit, or evade antiviral hosts defenses (3). An important challenge in the field is to decipher which of all the variants that appear should be monitored to implement measures that mitigate their risk to public health.

Mutations in SARS-CoV-2 have been reported since the early stages of the coronavirus disease 2019 (COVID-19) epidemic (4–6). The most common mutations described are single nucleotide polymorphisms (SNPs) and small deletions (7–9). Genomic surveillance of mutations has been mostly focused on the spike (S) protein because of its key role in viral entry and immunity (10), as well as the fact that this protein constitutes the basis of numerous SARS-CoV-2 vaccines (11). S is a homotrimeric protein whose heavily glycosylated ectodomain protrudes from the viral membrane, showing a bat-like shape with an N-terminal globular head connected to the membrane by an elongated stalk (12). The S protein is proteolytically processed by the cellular furin protease into the S1 and S2 subunits (13, 14). Additional proteolytic cleavage occurs following the binding of the S protein to host receptors, facilitating S1 subunit release. The C-terminal S2 subunit remains trimeric in the viral membrane but undergoes conformational changes that promote fusion with the host cell (15).

The first mutation identified as potentially concerning was a change from aspartic acid to glycine in the S1 subunit of the S protein at position 614 (S:D614G). S:D614G emerged early in the epidemic, becoming predominant in most countries within 2 months, and completely dominated the epidemic by August 2020 (16). As with any mutant, the initial spread of this mutation could have resulted from stochastic events, the dynamics of the epidemic, or an intrinsically higher viral fitness. More than 6 months after the initial report of this mutation, several studies reported evidence in favor of higher transmission efficacy in animal models and human populations (4, 17–19). S:D614G replicates better in some cell culture and animal models (17, 18, 20) and is associated with higher viral loads in infected individuals (16); importantly, however, it does not impact diagnostics or vaccine efficacy.

Following the first wave of the pandemic, additional variants have been reported from many countries. Among the first of these changes associated with variants in the spike protein was the amino acid replacement S:A222V, located at the N-terminal domain (NTD) of the S1 subunit, which occurred in the background of S:D614G. The variant containing this change, termed 20E, was first sequenced in Spain and expanded throughout Europe (5). Other variants have been reported since, including the so-called

cluster 5 variant, which harbors a combination of 3 SNPs and a single deletion related to mink farms in Denmark (21). One of the SNPs is in the S protein of this variant, S:Y453F; it occurs in the receptor-binding domain (RBD) and may increase binding to cell receptors in mink (22). By late 2020 or early 2021, three variants of concern (VOC) were described, all of which share the S:N501Y amino acid replacement in the RBD of the S protein: Alpha (also called 20I/501Y.V1 or lineage B.1.1.7) was originally described in the United Kingdom (9), Beta (20H/501Y.V2; B.1.351) in South Africa, and Gamma (20J/501Y.V3; P.1) in Brazil. Recently, in March 2021, a new VOC known as Delta (21A/478K.V1, B.1.617.2) emerged in India. The Delta variant does not contain S:501Y (23) and is displacing the predominant variant, Alpha (24). These variants are of particular concern because of their rapid spread, likely due to increased transmissibility (25–27). Reduction in neutralization has been found in different amino acids of the spike protein. VOC with the amino acid replacement S:N501Y (Alpha, Beta, and Gamma) exhibit the highest impact on immune evasion, followed by lineages harboring S:L452R that include the Delta variant (B.1.617.2) (28). While the effect of these variants on the immune response in convalescent and vaccinated individuals is still unclear, current data do not provide evidence of immune escape or compromising vaccine efficacy (29). Nevertheless, new mutations could emerge that hamper efforts to control the epidemic at regional or global scales by increasing transmissibility and/or reducing vaccine efficacy in the future.

The dominance of a lineage in a geographical region is sometimes determined by the number of introductions and mobility among regions (30) rather than by a change in a biological trait that confers a selective advantage (5). Nearly all VOC thus far have spread outside the country where they were initially identified and are estimated to spread faster than other cocirculating genotypes, becoming dominant for a period (25, 31, 32) and eventually being replaced locally by other variants (24). The current work describes the workflow for investigating the risk of emerging mutations in the spike protein of SARS-CoV-2, starting from genomic epidemiology and leading up to a biological and immunological characterization of SARS-CoV-2 mutations in terms of viral infectivity, virion stability, and neutralization by sera from convalescent and vaccinated individuals.

RESULTS

Multiple and independent mutations in amino acid positions 1163 and 1167 of the spike protein. SARS-CoV-2 genetic variation has been monitored by the Spanish sequencing consortium SeqCOVID to follow the expansion of mutations that could potentially result in a change of the biological properties of the virus. We focused on mutations in the S protein because of its relevance for infection and immunity (10). We detected two mutations in the S gene: G25049T (S:D1163Y) and G25062T (S:G1167V), which appeared in Spain as early as March and April 2020, respectively (see Fig. S1 in the supplemental material). These mutations continued arising independently of each other and, by the end of June, when the predominant circulating genotypes from the first wave in Spain had already been replaced by other variants (30), were also observed together (Fig. S1). Both positions have mutated multiple times independently and to different amino acids at a lower frequency. On the one hand, S:D1163 appears to have mutated at least 99 times (S:D1163Y, 84; S:D1163V, 4; S:D1163G, 3; S:D1163A, 2; S:D1163E, 2; S:D1163H, 2; S:D1163N, 1; and S:D1163H/Y, 1) in 47 lineages according to the pangolin scheme (33). On the other hand, S:G1167 appears to have mutated at least 54 times (S:G1167V, 39; S:G1167D, 4; S:G1167C, 3; S:G1167R, 3; S:G1167S, 3; S:G1167F, 1; and S:G1167A, 1) in 20 PANGO lineages, including B.1 (Fig. S2e) and its derivatives B.26, B.40 (Fig. S2c), and D.2 (Fig. S2f).

Clusters of transmission with amino acid changes in positions 1163 and 1167 of spike. The majority of mutated sequences in position 1163 and 1167 in the S protein (94.43%) were found in transmission clusters (see Materials and Methods for the definition of clusters) (Fig. 1a and b), with a small minority not belonging to a transmission cluster due to either incomplete sampling or failure to spread. While different amino acid changes have been detected at both positions, only one change at each position

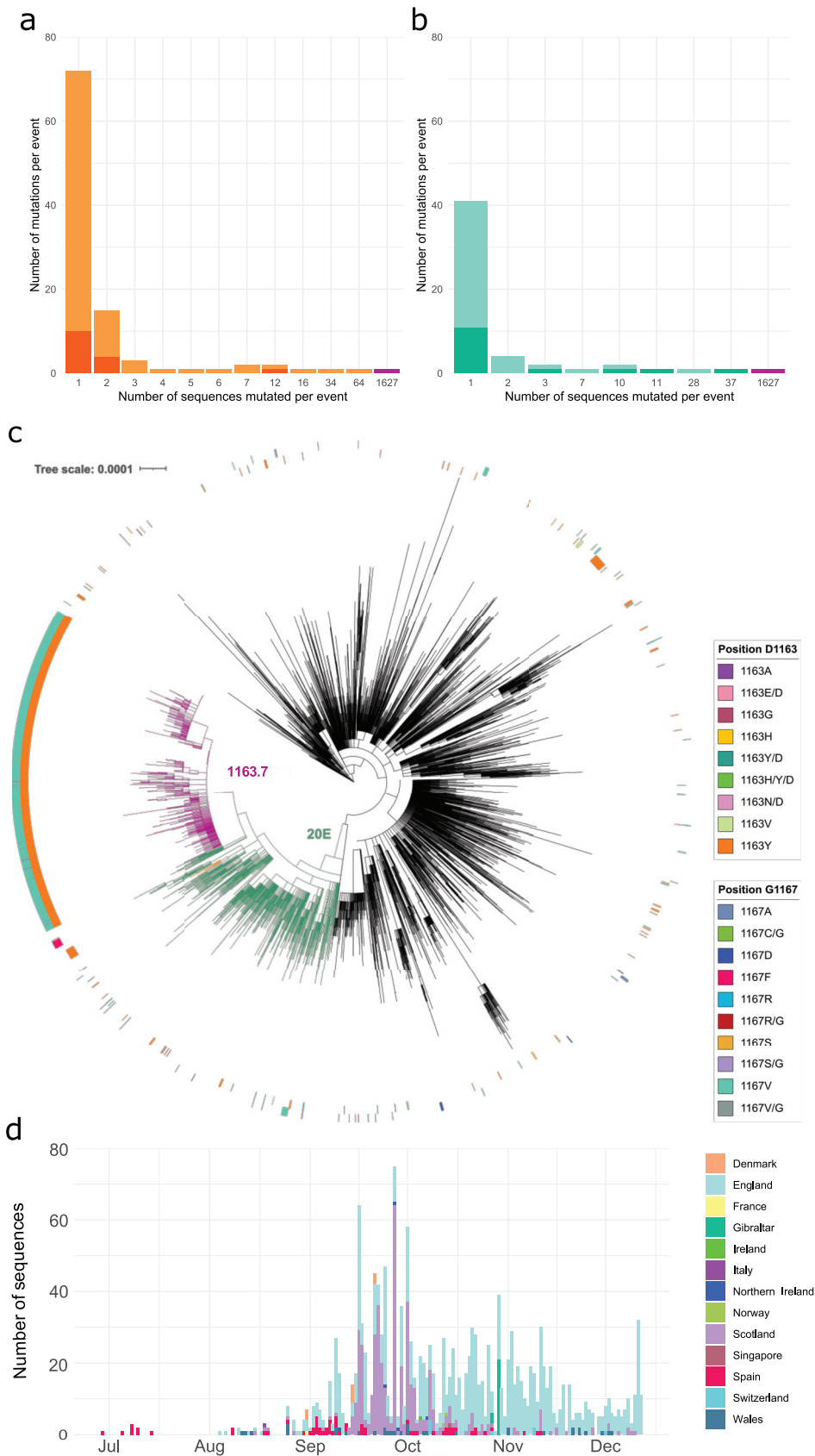


FIG 1 Sequences mutated at positions 1163 and 1167 of the S protein. (a) The number of mutation events for amino acid replacement S:D1163Y (light orange) or another S:D1163 amino acid replacements (dark orange) (Continued on next page)

appeared in most clusters: S:D1163Y in 83.33% and S:G1167V in 69.23% of clusters. S:D1163Y appeared in 22 transmission clusters (Fig. 1a) and S:G1167V in 8 clusters (Fig. 1b). Interestingly, the largest cluster included both the S:D1163Y and S:G1167V amino acid replacements together and was detected initially in 65 sequences from Spain until December 2020, representing 1.17% of the Spanish sequences and 1,627 sequences in total, representing 0.60% of sequences globally (Fig. 1c and d). The 1,627 sequences form a monophyletic cluster within lineage 20E (also described as 20E.EU1 [5] and B.1.177 [33]), which we designate cluster 1163.7. Cluster 1163.7 is characterized by nine nonsynonymous and six synonymous mutations with respect to the reference sequence from Wuhan (Table S2) but lacks any shared deletions. The amino acid changes A222V, D614G, D1163Y, and G1167V were found in the S protein, A220V and P365S were found in the N protein, V30L was found in ORF10, L67F was found in ORF14, and P4715L was found in ORF1ab (Fig. S3 and Table S2). Synonymous mutations were also observed in the ORF1ab, N, and M genes (Fig. S3 and Table S2).

Within 20E, the second largest cluster including any of these mutations was observed in 34 sequences with E654Q and D1163Y in S protein plus an additional 7 nonsynonymous and 6 synonymous mutations (Table S2 and Fig. S3). We designate this second cluster, which is also embedded within lineage 20E, cluster 1163.654 (Fig. 1c and Fig. S3). Cluster 1163.654 appeared first in Ireland on 23 July 2020 and subsequently appeared in Spain and England. However, cluster 1163.654 was no longer detected after 3 months.

Because of the risk posed by VOC (9, 32, 35), we examined whether mutations involving 1163 and 1167 of the S protein were observed in VOC until July 2021. We detected one of the mutations in 170 Delta, 676 Alpha, 147 Beta, and 153 Gamma sequences. Interestingly, S:D1163Y and S:G1167V were observed together in only one individual with 20I, the Alpha variant, although both positions showed polymorphism within the individual (relative frequency of 27% and 17% of the reads with S:D1163Y and S:G1167V, respectively).

Evolution of 1163.7. We explored the emergence and evolution of 1163.7, the largest and most successful cluster involving amino acid changes in positions 1163 and 1167 of the S protein. 1163.7 appeared in Spain in June 2020 in sequences from the Basque Country (Fig. 1d and Video S1) and subsequently appeared in individuals from other countries, accounting for a total of 1,627 sequences in GISAID (0.60% of 270,869 analyzed sequences by 23 December 2020) (Fig. 1d and Video S1). The majority of the 1163.7 sequences were obtained from the United Kingdom, including England ($n = 1,058$), Scotland ($n = 419$), Wales ($n = 34$), and Northern Ireland (5) but were also observed in Gibraltar (24 sequences), indicating successful migration and transmission (Video S1). Although 1163.7 is not well represented in sequences from other countries, it has been found in multiple sequences from Denmark ($n = 9$), Switzerland ($n = 8$), and Norway ($n = 2$) and single sequences from Italy, France, Singapore, and Ireland. By the end of 2020, 1163.7 was still circulating in Europe (Fig. 1d and Video S1), and it was represented by 1,923 sequences in GISAID by the end of February 2021 (0.33% of submitted sequences). After this time point, when VOC were increasing in frequency, 1163.7 ceased to be detected (Fig. 2), being replaced by the Alpha variant similarly to other variants in Europe, such as 20E.

Within 1163.7, we detected additional SNPs in individual sequences or small groups of sequences. One of these changes is E484K in the RDB of the S protein, a mutation

FIG 1 Legend (Continued)

orange). (b) The number of mutation events for amino acid replacement S:G1167V (light turquoise) or another S:G1167 amino acid replacements (dark turquoise). Bars in magenta indicate the appearance of both the S:D1163Y and S:G1167V amino acid replacements in the same sequences. (c) Maximum-likelihood phylogeny of 10,450 SARS-CoV-2 genomes. The inner ring represents sequences with amino acid changes in position D1163 of the S protein. The outer ring represents sequences with amino acid changes in position G1167 of the S protein. Branches are colored in magenta for 1163.7, green for clade 20E, and orange for cluster 1163.654. The scale bar indicates the number of nucleotide substitutions per site. (d) Temporal distribution and frequency of sequences with variant 1163.7 colored by geographical origin.

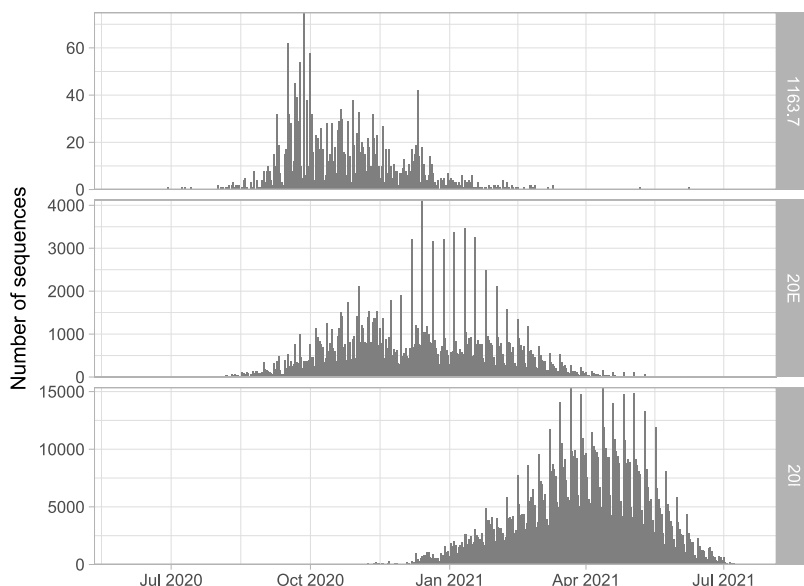


FIG 2 Temporal distribution of sequences in GISAID per variant. Number of sequences classified as cluster 1163.7 ($n = 2,106$), 20E ($n = 159,450$), and 20I ($n = 979,013$) by date from June 2020 until the beginning of July 2021.

present in three VOC (Alpha, Beta, and Gamma) that is implicated in increased ACE2 binding (36) and reduced neutralization by antibodies (37). In addition, we found another change associated with evasion of antibody immunity: a deletion of positions 141 to 144 in the S protein, which partially overlaps a smaller deletion at 144 reported in VOC Alpha (38). This subcluster included five sequences during January of 2021 from England and Wales (Table S2). The five sequences formed a monophyletic group embedded in 1163.7 (Fig. S5), identified as cluster 1163.7.V2, which displays other non-synonymous and synonymous mutations (Table S2), and only two sites are polymorphic within 1163.7.V2.

Positions 1163 and 1167 of the S protein are located in the heptad repeat 2 motif.

The S protein mediates both binding to cellular receptors and entry into the host cells (10). For the former, the RBD motif in the S1 subunit interacts with the cellular receptor in the prefusion state. In the postfusion state, two heptad repeat sequences (HR1 and HR2) in the S2 subunit must form a six-helix bundle in order to bring the viral and cellular membrane into close proximity (39, 40) (Fig. 3). S protein positions 1163 and 1167 are both located within the HR2 domain. Specifically, 1167 is present at the beginning of the HR2 motif and 1163 in its upstream linker region (Fig. 3a). Interestingly, this motif is highly invariable, showing 100% conservation across 14 viruses in the subgenus *Sarbecovirus*, to which SARS-CoV-2 belongs (Table S1) (41, 42). Structural characterization of the full-length ectodomain of S protein has shown that the stalk portion encompassing positions 1163 and 1167 presents intrinsic flexibility in the prefusion state (43), precluding its atomic visualization. This was recently confirmed by high-resolution cryo-electron tomographic reconstitution of SARS-CoV-2 (12), where this region was observed to constitute a flexible hinge that acts as a “knee”, connecting two helical coiled-coil regions of the stalk (upper and lower legs) (Fig. 3b). Within this structure, the conformational freedom provided by the glycine residue at position 1167 should play a key role in the flexibility of the knee. In contrast, in the postfusion state, this region shows high rigidity due to a strong structural rearrangement of the HR2 motif, which adopts an extended conformation and tightly packs along the central 3-helix bundle stem formed by the HR1 motif (Fig. 3c). The resulting HR1-HR2 bundle plays a key role in the mechanism of viral-host membrane fusion (43, 44), and mutations in this region could have a significant impact on the function of the S protein. In

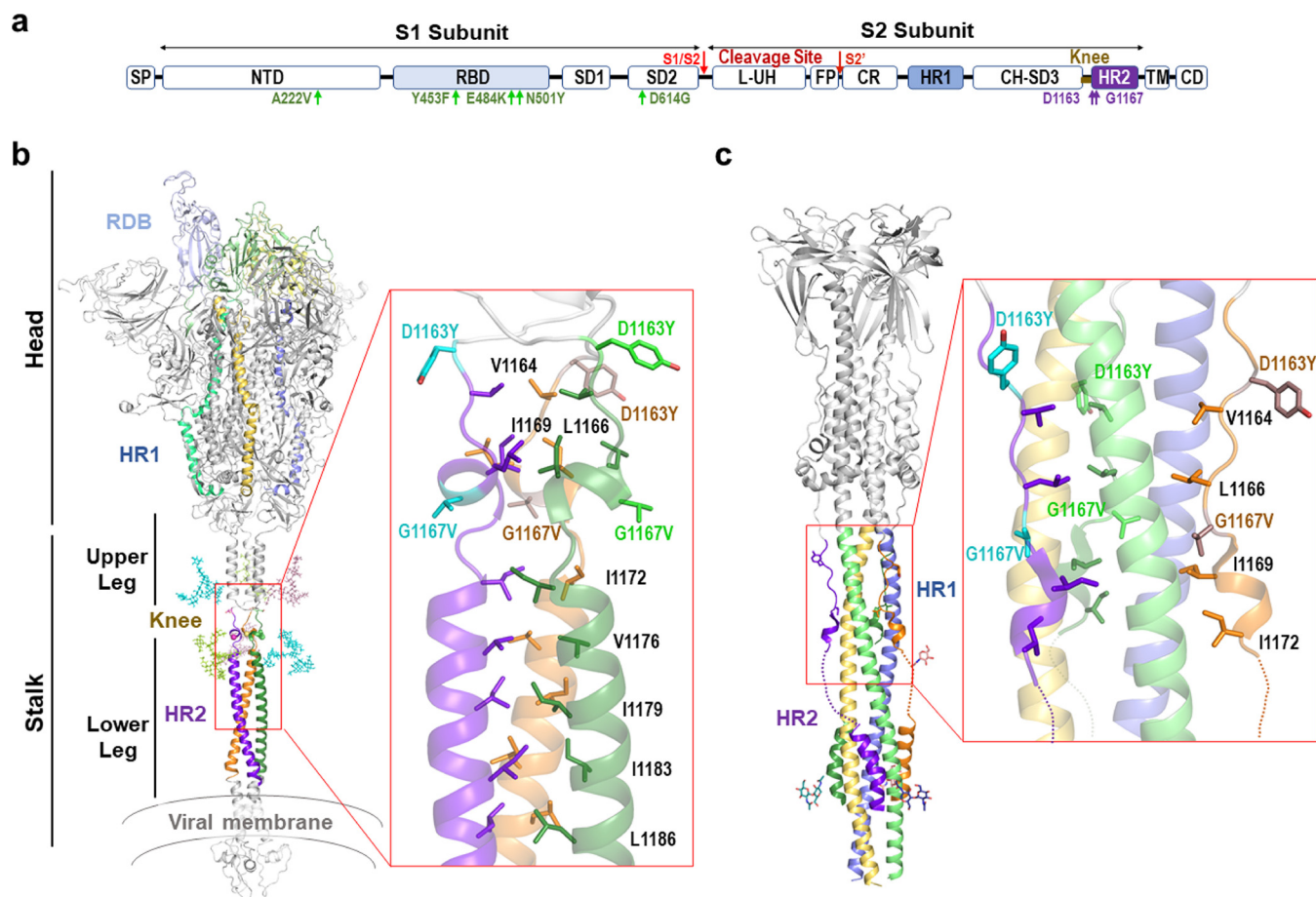


FIG 3 Structure of 1163 and 1167 in the pre- and postfusion states of S protein. (a) Schematic representation of the S protein. SP, signal peptide; NTD, N-terminal domain; RBD, receptor-binding domain; SD1 and SD2, subdomains 1 and 2; L-UH, linker-upstream helix; FP, fusion peptide; CR, connecting region; HR1, heptad repeat 1; CH-SD3, central helix subdomain 3; BH, β -hairpin; HR2, heptad repeat 2; TM, transmembrane; CD, cytoplasmic domain. Amino acid changes D1163Y and G1167V are indicated in purple, and other mutations described in the text are in green. (b) (Left) Cartoon representation of a structural model of prefusion membrane-bound trimeric S protein (77). In each subunit, the RBD, HR1, and HR2 domains are colored in different tones (light to dark) of blue, yellow, and green. The N-glycosylation of N1155 and N1176 is shown in stick representation and colored as the corresponding subunit. Functional and structural regions are marked. (Right) Close-up view of the N-terminal portion of HR2 where D1163Y and G1167V amino acid replacements are found. The side chains of mutated and hydrophobic residues in the HR2 region are shown in stick representation and colored as the corresponding subunit (mutated residues in a lighter tone). (c) Cartoon representation (left) of S2 subunit in postfusion conformation with HR1 and HR2 regions colored as in panel b and N-glycosylation around mutation position shown as sticks. (Right) Close-up view of the region encompassing the mutations (right), showing in stick representation the mutated and hydrophobic residues from the HR2 region shown in panel b. Dotted lines highlight HR2 disordered regions in the cryo-electron microscopy structure.

addition, the HR2 region is highly glycosylated, with this modification being regularly spaced in both the pre- and postfusion states and mostly aligning to the side of the helix bundle (12, 43, 44). Of note, two of these branched sugars are placed at positions N1158 and N1173, shielding positions 1163 and 1167 (Fig. 3b). Therefore, changes in stalk flexibility might have relevance in immunity by influencing both the intrinsic degree of exposure of this region and its sugar shielding.

Using the available structural information of the S protein in the pre- and postfusion conformations (43), we examined the possible implications of these mutations to viral infectivity. Based on these structures, G1167V amino acid replacement is predicted to confer significant rigidity to the structure in two ways. First, the introduction of a side chain strongly reduces the conformational freedom provided by the glycine residue. Second, the presence of the new aliphatic side chain provided by the valine residue strongly increases hydrophobicity, likely promoting the burial of this side chain in the HR1 helix 3-bundle stem in the postfusion state or favoring its integration in the neighbor helical coiled-coil in the prefusion state (Fig. 3b and c). Unlike position 1163,

position 1167 is fully exposed to the solvent in both the pre- and postfusion states (Fig. 3b and c). Hence, the effect of D1163Y is likely to stem from a change in the nature of the side chain, switching from a charged aspartic acid residue at physiological pH to a polar group with hydrophobic properties in the tyrosine.

Spike amino acid changes D1163Y and G1167V do not increase viral infectivity.

Previous reports have indicated that mutations in the S protein can increase infectivity (4, 18, 45–47). Because the biggest transmission cluster for amino acid changes in S positions 1163 and 1167 corresponds to the double mutation D1163Y/G1167V (characteristic of 1163.7), we explored whether these amino acid changes in combination influence infectivity. For this, we pseudotyped vesicular stomatitis virus lacking its glycoprotein and encoding green fluorescent protein (48) (VSVΔG-GFP) with different S genotypes: (i) Wuhan S genotype (the reference sequence from Wuhan encoding S: D614), (ii) Wuhan S genotype with S:D614G, (iii) S genotype common in 20E sequences characterized by S:A222V and S:D614G, and (iv) cluster 1163.7 (characterized by S: A222V, S:D614G, S:D1163Y, and S:G1167V). Infectious virus production was then assessed by limiting dilution and counting of GFP-positive cells in both Vero and A549-hACE2-TMPRSS2 cells. As previously reported (16, 18, 49), the 20E S genotype enhanced infectivity relative to the D614 S genotype by 70% in both Vero cells ($P = 0.005$ by unpaired t test) (Fig. 4a) and A549-hACE2-TMPRSS2 cells ($P = 0.016$ by unpaired t test) (Fig. 4b). The 20E S genotype also showed a trend toward increased infectivity versus the S:D614G replacement alone (35% increase in both cell lines), as previously reported (47), yet the difference was not statistically significant ($P = 0.2$ by unpaired t test) (Fig. 4a and b). In contrast, the 1163.7 S genotype significantly diminished virus infectivity versus the 20E genotype, reducing virus titers by 20% in Vero cells ($P = 0.009$ by unpaired t test) (Fig. 4a) and 29% in A549-hACE2-TMPRSS2 cells ($P = 0.03$ by unpaired t test) (Fig. 4b). This is in agreement with a potential stabilization of the HR2 helix (Fig. 3), which should limit the ability of the S protein to sample different structural conformations that might be required for binding host receptors. Hence, the 1163.7 S genotype does not increase infectivity *in vitro*.

To corroborate that the 1163.7 S genotype does not show higher infectivity *in vivo*, we tested if individuals infected with 1163.7 had higher viral loads. For this, we used the cycle threshold (C_T) of real-time PCR used for diagnosis as a surrogate. As previously reported (16), we detected higher C_T values for the D614 wild-type variant (mean $C_T = 27.00$) than for genotypes encoding S:D614G (C_T mean = 25.32; $P < 0.01$ by unpaired Wilcoxon test) (Fig. 4c). We did not find significant differences in viral loads between individuals infected with the 1163.7 genotype and other genotypes within 20E (mean $C_T = 21.14$ versus 20.63; $P = 0.72$ by unpaired Wilcoxon test) (Fig. 4c), in agreement with the lack of infectivity advantage observed *in vitro*. Interestingly, higher viral loads were observed in individuals infected with 1163.7 and other 20E viruses (S: A222V and S:D614G) than the S:D614G virus alone (S:D614G mean $C_T = 25.32$; 20E mean $C_T = 21.14$; 1163.7 mean $C_T = 20.63$; $P < 0.01$ for both comparisons by unpaired Wilcoxon test) (Fig. 4c).

Amino acid changes D1163Y and G1167V do not alter S protein stability. As increased spike stability could impact transmissibility by maintaining virion infectivity during the intrahost transmission period, we assessed the temperature sensitivity of the different S variants. For this, we subjected VSV particles pseudotyped with different S genotypes to a range of temperatures for 15 min, after which we evaluated the surviving fraction. Overall, no major differences in the degree to which the different S proteins lost infectivity upon heat exposure were observed, with all S proteins showing a 50% reduction in infectivity at a similar temperature range (39.8 to 42.2°C; $P > 0.05$ for all except Wuhan S genotype [D614] versus 20E S genotype [S:A222V and S:D614G], where P is 0.01) (Fig. 4d).

S:D1163Y and S:G1167V modestly reduce sensitivity to neutralization by existing antibody immunity. Positions 1163 and 1167 of the S protein have been reported to occur in both T- and B-cell SARS-CoV-2 epitopes (50–52). Moreover, numerous studies have shown that mutations in the S protein can affect antibody neutralization (53, 54).

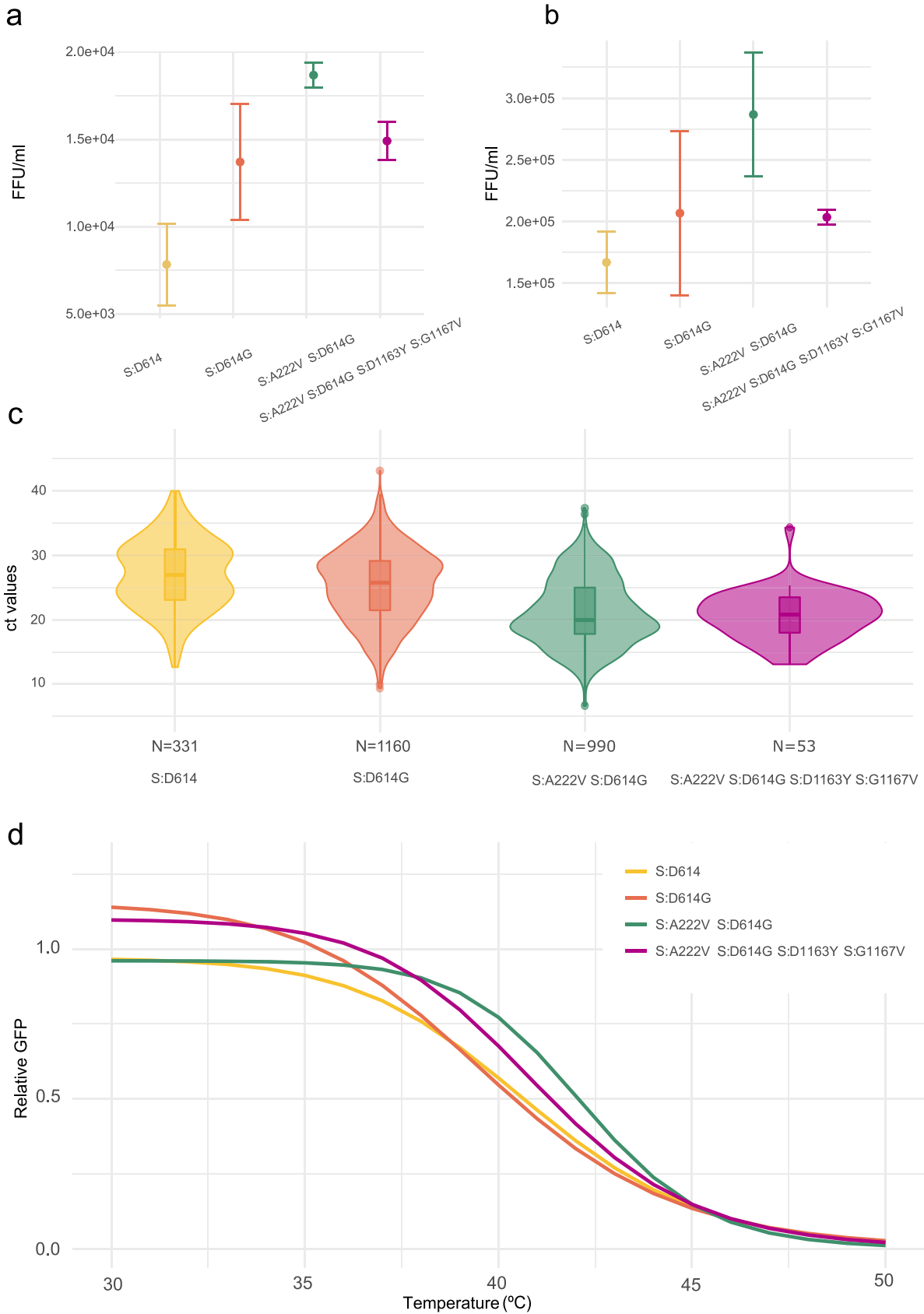


FIG 4 Comparison of the infectivity and stability of different S genotypes. (a and b) The infectivity of VSV particles pseudotyped with each S protein genotype in either Vero cells (a) or human A549 cells expressing ACE2 and TMPRSS2 (b). Means and standard deviations for three (Continued on next page)

We therefore examined if the presence of D1163Y and G1167V alters the neutralization capacity of convalescent-phase sera using VSV pseudotyped with either the 20E or 1163.7 S genotypes. We tested the sensitivity of these pseudotyped viruses to neutralization by sera from early (April 2020; first wave in Spain) or later (October 2020; second wave in Spain) in the pandemic, when newer variants were dominant (5, 30). Overall, the 1163.7 genotype conferred a modest but statistically significant reduction in sensitivity to neutralization by six serum samples tested from the early stage of the pandemic, as measured by the titers required to inhibit viral entry by 80% (ID_{80} ; mean = 6.75; range, 1.30 to 17.68; $P = 0.008$ by paired t test) (Fig. 5a). A statistically significant but smaller effect was observed when the titers required to inhibit viral entry by 50% were examined (ID_{50} ; mean = 2.27; range, 1.61 to 3.54; $P < 0.001$ by paired t test) (Fig. 5b). In contrast, both 20E and 1163.7 were equally susceptible to sera from patients infected during the second wave (ID_{80} ; mean = 1.03; range, 0.87 to 1.23; $P = 0.83$ by paired t test) (Fig. 5b). As a modest reduction in titers was observed with sera from early in the pandemic (Fig. 5a), when the S genotype of circulating viruses was more similar to the one present in currently approved vaccines (55, 56), we examined if the 1163.7 S genotype resulted in reduced neutralization by sera from donors vaccinated with the BNT162b2 vaccine. No significant differences in susceptibility to antibody neutralization from vaccinated donors were observed between the two genotypes (Fig. 5c).

DISCUSSION

SARS-CoV-2 success is linked to its ability to infect and be transmitted. Mutations that emerge independently several times and increase in frequency are likely to confer enhanced viral infectivity, transmission, or immune evasion. The identification of such mutants is of great importance, as they can significantly impact public health. On the other hand, the appearance of mutations can also be driven by stochastic events, and the ability to evaluate the potential risk posed by new variants is of key importance to appropriately tailor public health responses. In this work, we identified two amino acid replacements at positions 1163 and 1167 of the S protein that appeared to be potentially beneficial for the virus based on several lines of evidence. First, these mutations are highly variable within SARS-CoV-2 but conserved across the closely related coronaviruses. Second, the vast majority of sequences harboring these mutations appeared in clusters (Fig. 1a and b). Third, both positions have been reported as positively selected multiple times throughout the SARS-CoV-2 phylogeny indicating a fitness advantage (57). Finally, the largest cluster containing either of these mutations, and therefore the most successful in terms of transmission, harbored both mutations together (Fig. 1a and b). This infection cluster was sustained for more than 6 months across Europe, suggesting that both mutations together could increase viral fitness.

For these reasons, we conducted a series of experiments to assess whether the two mutations conferred a biological advantage to the virus *in vitro*. Analysis of the mutation in the context of available structures suggested that G1167V could alter the flexibility of the S protein stalk by both restricting the conformational freedom normally conferred by the wild-type glycine residue and by introducing a hydrophobic side chain that will favor burial in the HR2 coiled-coil leucine zipper of the prefusion state (Fig. 3). This extensive flexibility of the S prefusion stalk seems to be unique to the SARS-CoV-2 (43) and has been suggested to increase avidity for the host receptors by allowing the engagement of multiple S proteins (43). Therefore, stalk stabilization by

FIG 4 Legend (Continued)

replicates are plotted. (c) Comparison of cycle threshold (C_t) values for the N gene from patients infected with viruses encoding different S protein variants. Data are derived from 2,534 sequences from the SeqCOVID consortium. The number of observations (N) analyzed for each genotype is indicated. (d) The thermal sensitivity of VSV pseudotyped with different S genotypes following incubation at 15 min. Data are standardized to the surviving fraction following incubation at 30°C, and the three-parameter log-logistic equation is plotted. FFU, focus forming units.

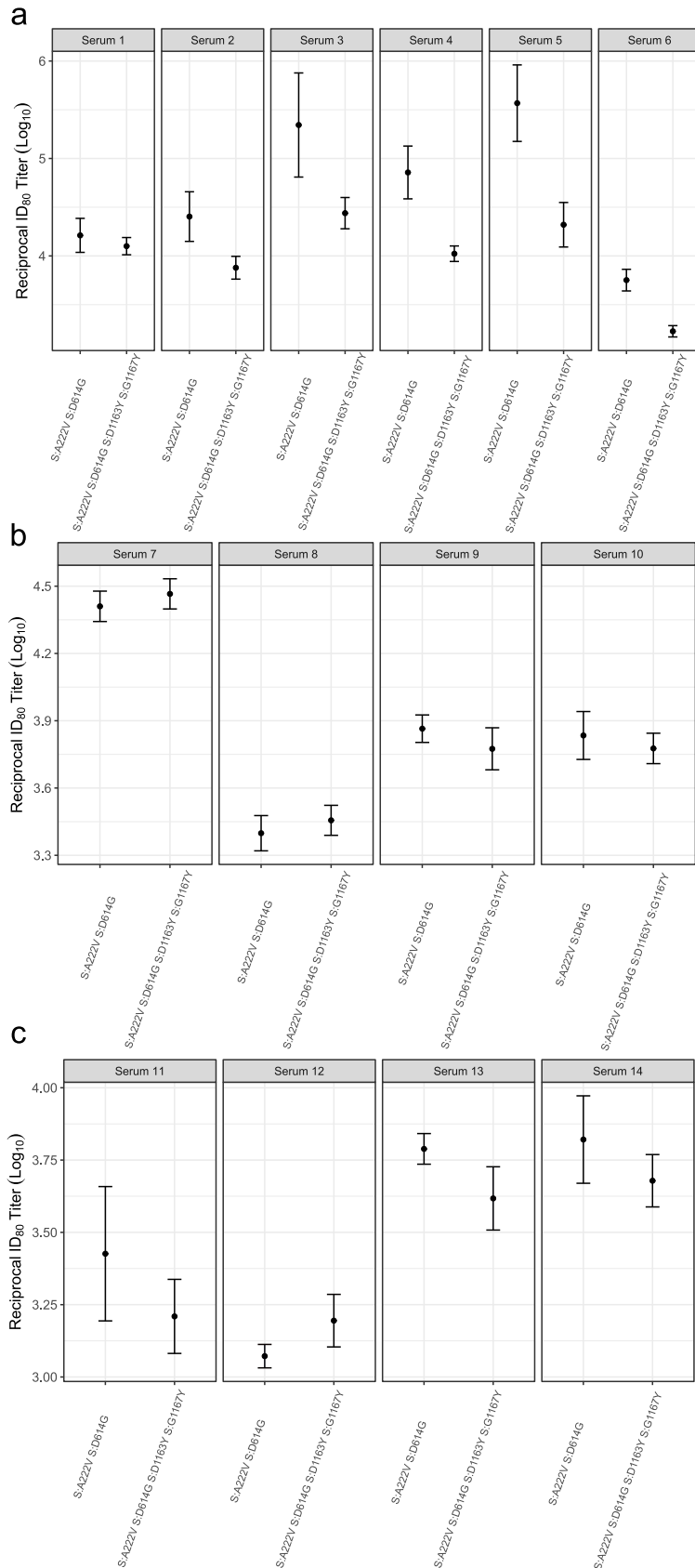


FIG 5 Antibody neutralization of 20E and 1163.7 variants. The reciprocal titer at which infection with the 20E S genotype (S:A222V and S:D614G) or 1163.7 S genotype (20E plus S:D1163Y and S:G1167V) (Continued on next page)

G1167V is likely to result in a reduced ability of S to bind receptors in the target cell. In agreement with this, we found reduced infectivity upon introduction of both changes D1163Y and G1167V into the spike protein (Fig. 4a and b). In addition, we found no indication of resistance to heat inactivation that could facilitate environmental transition between hosts (Fig. 4c), and the viral load in clinical specimens showed no difference due to the presence of these two mutations compared to the 20E S genotype (Fig. 4d).

We examined if these two mutations conferred evasion of preexisting immunity, which could compromise vaccine efficacy and/or result in reinfection. For this, we used sera from both the first (April 2020) and second (October 2020) epidemic waves of the infection in Spain, because an almost complete replacement of SARS-CoV-2 S genotypes of different variants occurred between these two time points in Spain (30). When utilizing sera from donors infected during the first wave of the pandemic in Spain, we found a modest but statistically significant reduction in susceptibility to neutralization of the 1163.7 S genotype compared to the 20E S genotype of approximately 6-fold (Fig. 5a). However, no difference in neutralization was observed between the two variants when sera from patients infected during the second wave were used (Fig. 5b). Overall, the magnitude of the observed reduction in neutralization susceptibility to sera from individuals infected during the first wave was much less pronounced than that observed for other genotypes implicated in immune evasion (54), although the degree of reduced neutralization required to confer a biologically relevant fitness advantage *in vivo* has not been established. Importantly, we also found no evidence for reduced neutralization of the 1163.7 variant by sera from donors immunized with the BNT162b2 vaccine (Fig. 5c). Since all currently available vaccines, including BNT162b2, are based on the Wuhan S genotype, it is expected that these mutations will not reduce the effectiveness of the other vaccines either.

Both S amino acid positions 1163 and 1167 are embedded in experimentally confirmed T- and B-cell epitopes. Interestingly, for T-cell epitopes, a predicted HLA-II epitope including positions 1163 and 1167 has been experimentally verified to bind to HLA DRB1*01:01, the prototype molecule for the DR supertype (epitope identifier in Immune Epitope DataBase: 9006 [58]). Additionally, amino acid S:D1163 is included in a SARS-CoV-2 T-cell linear epitope eliciting T-cell responses in convalescent COVID-19 cases (59) as well as in SARS-CoV-2-naïve individuals (52), indicating cross-reactivity in epitopes involving these regions. B-cell linear epitopes that span D1163 and G1167 have also been reported (51), with D1163 belonging to a dominant linear B-cell epitope recognized by more than 40% COVID-19 patients used in the assay (53). Hence, it is possible that these mutations could play a role in modulating T-cell responses. However, at the time cluster 1163.7 appeared and transmitted in Europe, large-scale vaccination had not been implemented and the majority of the population had not been infected by SARS-CoV-2. Therefore, there was likely little selection of SARS-CoV-2 variants that evade existing immunity.

Overall, clinical and experimental data do not support the idea that D1163Y and G1167V in the S protein confer temperature resistance, higher infectivity *in vitro*, higher viral load *in vivo*, or significant escape from antibody neutralization. The biological consequences of these mutations are therefore unlikely to confer a significant fitness advantage. Indeed, these early findings are in agreement with the subsequent observation that these mutations ceased to circulate in Europe as VOC Alpha increased in frequency.

MATERIALS AND METHODS

Whole-genome sequencing and genome assembly of SeqCOVID consortium sequences. A total of 5,017 clinical samples were received, sequenced, and analyzed by the SeqCOVID consortium from all

FIG 5 Legend (Continued)

is reduced by 80% (ID_{80}) by sera from individuals infected during the early stage of the pandemic (a) or during a later stage of the pandemic (b) and from donors vaccinated with the BNT162b2 vaccine (c). The means and standard errors for three replicates are plotted.

autonomous communities of Spain. These samples were confirmed as SARS-CoV-2 positive by reverse transcription-PCR (RT-PCR) carried out by clinical microbiology services from each hospital. All sequences are available at GISAID under the accession numbers detailed in Table S1.

For sequencing, RNA samples were retrotranscribed into cDNA. SARS-CoV-2 complete genome amplification was performed in two multiplex PCRs, according to the protocol developed by the ARTIC network (60), using the V3 multiplex primer scheme (61). From this step, two amplicon pools were prepared, combined, and used for library preparation. The genomic libraries were constructed with the Nextera DNA Flex sample preparation kit (Illumina Inc., San Diego, CA) according to the manufacturer's protocol, with 5 cycles for indexing PCR. Whole-genome sequencing was performed in the MiSeq platform (2×200 cycles paired-end run; Illumina).

Reads obtained were processed through a bioinformatic pipeline based on iVar (58), available at <https://gitlab.com/fisabio-ngs/sars-cov2-mapping>. The first step in the pipeline removed human reads with Kraken (59); then, fastq files were filtered using fastp (62) v 0.20.1 (arguments employed: `-cut tail, -cut-window-size, -cut-mean-quality, -max_len1, -max_len2`). Finally, mapping and variant calling were performed with iVar v 1.2, and quality control assessment was carried out with MultiQC (63).

Analysis of the S gene of sarbecoviruses related to SARS-CoV-2. Fourteen sequences including SARS-CoV-2 belonging to sarbecoviruses, sequences were annotated with annotation files available in the NCBI database in order to locate the spike gene coordinates (accession numbers are available in Table S1). The 14 sequences harboring the S gene were concatenated and aligned with MEGA-X (64) using amino acids with the ClustalW algorithm with default options.

Sampling SARS-CoV-2 from non-Spanish consortium sequences. To build the global alignment, sequences were downloaded from GISAID including all the pandemic periods since the first known case sequenced (from 24 December 2019) until the last sample on 22 December 2020. We used two filters to select the data set: sequences with more than 29,000 bp, and sequences with known dates of sampling. Sequences downloaded from GISAID were aligned against the SARS-CoV-2 reference genome (65) using MAFFT (66), omitting all insertions and getting an alignment length of 29,903 bp. The final alignment constructed included 270,869 sequences, all sequences with GISAID ID used for this study are available in Table S1.

Frequency and detection of mutated positions. Single nucleotide variants were detected using the global data set alignment, generating a VCF file with SNP sites (67) v 2.5.1 (argument employed: `-v`), using the reference genome as the reference bases for detecting mutations. This VCF file was processed with a Python script to assess all mutated samples by position, calculating the frequencies of the global data set and annotating sequences with the detected mutations. After that, the mutated positions were annotated with snpEff (68) v 5.0 using SARS-CoV-2 reference database annotation (arguments employed: `-c, -noStats, -no-downstream, -no-upstream, NC_045512.2`).

Genotypes detected that involved mutations in 1163 and 1167 such as clusters 1163.7 and 163.654 were represented in a circos plot with the R package circlize (69) v 0.4.12.1004.

Alignments. For the phylogenetic analysis, a reduced data set was selected from the 270,869 sequences. Duplicated sequences were removed with seqkit v 0.13.2 (arguments employed: `rmdup -s`). A total of 8,397 sequences were selected at random with the same temporal distribution by month as the initial data set by Python scripting. The 8,397 sequences were concatenated with 2,053 sequences harboring amino acid replacements in D1163 and G1167 of the S protein, thus resulting in an alignment of 10,450 sequences (Table S1).

The data set to represent Alpha phylogenetic relationships included 3,067 randomly selected samples identified by the PANGO typing system (<https://github.com/cov-lineages/pangolin>) as 201 plus the 33 sequences with amino acid replacements in S:D1163 and/or S:G1167 (Table S1).

For all the alignments, problematic positions reported by Lanfear (70) were masked for the phylogenetic reconstruction using `masked_alignment.sh` script.

Phylogenetic analysis. Maximum-likelihood phylogenies in Fig. 1 and Fig. S2, S4, and S5 were reconstructed from the masked alignment using IQ-TREE (71) v 1.6.12 with GTR model and collapsing near-zero branches (arguments employed: `-czb, -m GTR`). The phylogenies were annotated and visualized with iTOL v 4 (72).

The phylogeny in Video S1, composed by 10,450 sequences, was built with the Nextstrain pipeline (<https://github.com/nextstrain/augur>) to monitor and visualize temporal and geographical transmission of 1163.7.

Clusters of transmission involving 1163 and 1167 S amino acid replacements. We used the phylogeny of 10,450 sequences enriched with all sequences mutated in 1163 and 1167 to quantify the minimum number of mutational events involving positions 1163 and 1167 in the S protein. We first defined which mutations characterize internal nodes using R packages: tidytree v 0.3.3 and treeio v 1.14.3 (73). We then depicted monophyletic clusters sharing at least one of the two mutations. Transmission clusters were defined as all sequences that (i) are derived from an internal node characterized by the same nucleotide mutation involving 1163 or 1167 amino acid replacements, (ii) include more than one sequence, and (iii) have the nucleotide mutation in at least 95% of sequences. Additionally, redundant nodes were eliminated, keeping the ancestral node of the cluster. Sequences with at least one mutation but not in clusters were counted as single events of mutation in the phylogeny.

Structural analysis of 1163 and 1167 S amino acid replacements. The atomic coordinates for S protein in prefusion state were retrieved from the CHARMM-GUI COVID-19 Archive (<http://www.charmm-gui.org/docs/archive/covid19>). The atomic coordinates for S protein in the postfusion state were retrieved from Protein Data Bank (PDB code 6XRA [43] and PDB code 6LXT [74]). Mutations were introduced using single mutation tool embedded in COOT (75), and figures were generated with PyMOL (www.pymol.org).

Production of SARS-CoV-2-pseudotyped vesicular stomatitis virus, titration, and thermal stability evaluation. Mutations were introduced into a plasmid encoding a codon-optimized S protein (14) by site directed mutagenesis (see Table S3 for primers). All mutations were verified by Sanger sequencing (see Table S3 for primers). To evaluate the efficiency of virus production, three transfections in HEK293 cells (CRL-1573 from ATCC) were performed for each plasmid to generate pseudotyped VSV harboring the indicated S protein (76). The titers of the virus produced were then assayed by serial dilution, followed by infection of either Vero cells (CCL-81 from ATCC) or A549 cells expressing ACE2 and TMPRSS2 (InvivoGen catalog code a549-hace2tpsa) and counting of GFP-positive cells (focus-forming units [FFU]) at 16 h postinfection. Statistical comparisons were performed by unpaired *t* test (R package: stats v 3.6.1) with normalized logarithmic data. For assessing thermal stability, 1,000 FFU (as measured on Vero cells) were incubated for 15 min at 30.4, 31.4, 33, 35.2, 38.2, 44.8, 47, 48.6, or 49.6°C before addition to Vero cells previously seeded in a 96-well plate (10,000 cells/well). GFP signal in each well was determined 16 h postinfection using an Incucyte S3 system (Essen Biosciences). The mean GFP signal observed in several mock-infected wells was subtracted from those of all infected wells, followed by standardization of the GFP signal to the mean GFP signal from wells incubated at 30.4°C. Finally, a three-parameter log-logistic function was fitted to the data using the drc package v 3.0-1 in R (LL.3 function), and the temperature resulting in 50% inhibition was calculated using the drc ED function. Statistical differences in the temperature resulting in 50% reduction of infection were evaluated using the drc EDcomp function.

Evaluation of neutralization by convalescent-phase sera and efficacy of virus particle production. Pseudotyped VSV virions bearing the 20E or 1163.7 S genotype were evaluated for sensitivity to neutralization by convalescent-phase sera as previously described (76). Briefly, 16 h postinfection, GFP signal in each well was determined using an Incucyte S3 system (Essen Biosciences). The mean GFP signal observed in several mock-infected wells was subtracted from that of all infected wells, followed by standardization of the GFP signal in each well infected with antibody-treated virus to that of the mean GFP signal from wells infected with mock-treated virus. Any negative values resulting from background subtraction were arbitrarily assigned a low, nonzero value (10^{-5}). The serum dilutions were then converted to their reciprocal, their logarithm (\log_{10}) was taken, and the dose resulting in 50% (ID_{50}) or 80% (ID_{80}) reduction in GFP signal was calculated in R using the drc package v 3.0-1. A two-parameter log-logistic regression (LL2 function) was used for all samples except when a three-parameter logistic regression provided a significant improvement to fit, as judged by the ANOVA function in the drc package (e.g., $P < 0.05$ following multiple-testing correction using the Bonferroni method). All first-wave samples were obtained from donors that were admitted to the intensive care unit and were collected during April 2020. For the second-wave donors, sera were obtained (October 2020) from patients with severe COVID-19 requiring inpatient treatment. Similarly, samples were obtained from immunized donors who had no history of SARS-CoV-2 infection and who had received a second dose of Pfizer-BioNTech COVID-19 vaccine (BNT162b2; February 2021). All vaccinated individuals tested negative for antibodies against the SARS-CoV-2 N protein using a dual-recognition immunochromatographic assay (INgezim COVID 19 CROM 50.CoV.K41; Eurofins Ingenasa).

Ethics approval and consent to participate. Sequencing of the samples was approved by the ethics committee Comité Ético de Investigación de Salud Pública y Centro Superior de Investigación en Salud Pública (CEI DGSP-CSISP), no. 20200414/05.

All samples from Hospital Universitario y Politécnico La Fe de Valencia were collected after informed written consent had been obtained, and the project was approved by the ethical committee and institutional review board (registration number 2020-123-1).

Data availability. All generated SARS-CoV-2 genomes from SeqCOVID consortium are available in the GISAID platform under the accession numbers available in Table S1. Code and data used are available at the GitHub repository (https://github.com/PathoGenOmics/1163.7_SARS-CoV-2).

SUPPLEMENTAL MATERIAL

Supplemental material is available online only.

VIDEO S1, MOV file, 1.6 MB.

FIG S1, PDF file, 0.2 MB.

FIG S2, PDF file, 2.3 MB.

FIG S3, PDF file, 0.2 MB.

FIG S4, PDF file, 0.1 MB.

FIG S5, PDF file, 0.04 MB.

FIG S6, PDF file, 0.1 MB.

TABLE S1, TXT file, 18.8 MB.

TABLE S2, XLSX file, 0.01 MB.

TABLE S3, XLSX file, 0.01 MB.

ACKNOWLEDGMENTS

We acknowledge the patients and the Consorcio Hospital General de Valencia Biobank integrated in the Valencian Biobanking Network for their collaboration, as well as the

patients and hospital staff at Hospital Universitario y Politécnico La Fe de Valencia. In addition, we thank Gert Zimmer (Institute of Virology and Immunology, Mittelhäusern/Switzerland), Stefan Pohlmann, and Markus Hoffmann (German Primate Center, Infection Biology Unit, Goettingen/Germany) for providing the reagents required for the generation of VSV-pseudotyped viruses and the codon-optimized S plasmid. We acknowledge all the efforts from different laboratories and authorities submitting all possible sequences of SARS-CoV-2 worldwide and making them available on the GISAID platform.

M.C. and R.G. are supported by Ramón y Cajal program from Ministerio de Ciencia. This research work was supported by the European Commission–NextGenerationEU, the Instituto de Salud Carlos III project COV20/00140 and COV20/00437 and the Generalitat Valenciana (SEJI/2019/011 and Covid_19-SCI). Action was cofinanced by the European Union through the Operational Program of the European Regional Development Fund (ERDF) of the Valencian Community 2014-2020.

P.R.-R.: Conceptualization, Methodology, Formal Analysis, Investigation, Visualization, Writing Original Draft. C.F.-G.: Conceptualization, Methodology, Formal Analysis, Review and edit draft. A.C.-O.: Formal Analysis, Review and edit draft. M.G.L.: Formal Analysis, Review and edit draft. S.J.-S.: Software, Validation, Review and edit draft. I.C.-M.: Methodology, Resources, Review and edit draft. P.R.-H.: Investigation, Review and edit draft. M.T.-P.: Methodology, Resources, Review and edit draft. M.A.B.: Investigation, Methodology, Review and edit draft. G.D.: Methodology, Software, Data Curation, Review and edit draft. L.M.-P.: Methodology, Project Administration, Review and edit draft. M.G.: Resources, Review and edit draft. M.M.-A.: Resources, Review and edit draft. M.D.G.: Resources, Review and edit draft. J.L.P.: Resources, Review and edit draft. F.G.-C.: Funding, Project Administration, Supervision, Review and edit draft. I.C.: Funding, Project Administration, Supervision, Review and edit draft. A.M.: Formal analysis, Writing Original Draft. R.G.: Conceptualization, Methodology, Formal Analysis, Writing Original Draft, Supervision, Funding. M.C.: Conceptualization, Methodology, Investigation, Formal Analysis, Writing Original Draft, Supervision, Funding.

SeqCOVID-SPAIN consortium members include the following: Iñaki Comas, Fernando González-Candelas, Galo A. Goig-Serrano, Álvaro Chiner-Oms, Irving Cancino-Muñoz, Mariana Gabriela López, Manoli Torres-Puente, Inmaculada Gómez, Santiago Jiménez-Serrano, Lidia Ruiz-Roldán, María Alma Bracho, Neris García-González, Llúcia Martínez Priego, Inmaculada Galán-Vendrell, Paula Ruiz-Hueso, Griselda De Marco, Ma Loreto Ferrús Abad, Sandra Carbó-Ramírez, Mireia Coscollá, Paula Ruiz Rodríguez, Giuseppe D'Auria, Francisco Javier Roig Sena, Hermelinda Vanaclocha Luna, Isabel San Martín Bastida, Daniel García Souto, Ana Pequeño Valtierra, Jose M. C. Tubio, Fco. Javier Temes Rodríguez, Jorge Rodríguez-Castro, Martín Santamarina García, Nuria Rabella Garcia, Ferrán Navarro Risueño, Elisenda Miró Cardona, Manuel Rodríguez-Iglesias, Fátima Galán-Sanchez, Salud Rodríguez-Pallares, María de Toro, María Pilar Bea-Escudero, José Manuel Azcona-Gutiérrez, Miriam Blasco-Alberdi, Alfredo Mayor, Alberto L. Garcia-Basteiro, Gemma Moncunill, Carlota Dobaño, Pau Cisteró, Oriol Mitjà, Camila González-Beiras, Martí Vall-Mayans, Marc Corbacho-Monné, Andrea Alemany, Darío García de Viedma, Laura Pérez-Lago, Marta Herranz, Jon Sicilia, Pilar Catalán, Julia Suárez, Patricia Muñoz, Cristina Muñoz-Cuevas, Guadalupe Rodríguez Rodríguez, Juan Alberola Enguídanos, Jose Miguel Nogueira Coito, Juan José Camarena Miñana, Antonio Rezusta López, Alexander Trstancho Baró, Ana Milagro Beamonte, Nieves Martínez Cameo, Yolanda Gracia Grataloup, Elisa Martró, Antoni E. Bordoy, Anna Not, Adrián Antuori, Anabel Fernández, Nona Romani, Rafael Benito Ruesca, Sonia Algarate Cajo, Jessica Bueno Sancho, Jose Luis del Pozo, Jose Antonio Boga Riveiro, Cristián Castelló Abietar, Susana Rojo Alba, Marta Elena Álvarez Argüelles, Santiago Melón García, Maitane Aranzamendi Zaldumbide, Óscar Martínez Expósito, Mikel Gallego Rodrigo, Maialen Larrea Ayo, Nerea Antona Urieta, Andrea Vergara Gómez, Miguel J. Martínez Yoldi, Jordi Vila Estapé, Elisa Rubio García, Aida Peiró-Mestres, Jessica Navero-Castillejos, David Posada, Diana Valverde, Nuria Estévez-Gómez, Iria Fernández-Silva, Loretta de

Chiara, Pilar Gallego-García, Nair Varela, Rosario Moreno Muñoz, Ma Dolores Tirado Balaguer, Ulises Gómez-Pinedo, Mónica Gozalo Margüello, Ma Eliecer Cano García, José Manuel Méndez Legaza, Jesús Rodríguez Lozano, María Siller Ruiz, Daniel Pablo Marcos, Antonio Oliver, Jordi Reina, Carla López-Causapé, Andrés Canut Blasco, Silvia Hernáez Crespo, Ma Luz Cordón Rodríguez, Ma Concepción Lecaroz Agara, Carmen Gómez González, Amaia Aguirre Quiñonero, José Israel López Mirones, Marina Fernández Torres, Ma Rosario Almela Ferrer, José Antonio Lepe Jiménez, Verónica González Galán, Ángel Rodríguez Villodres, Nieves Gonzalo Jiménez, Ma Montserrat Ruiz García, Antonio Galiana Cabrera, Judith Sánchez-Almendo, Gustavo Cilla Eguiluz, Milagrosa Montes Ros, Luis Piñeiro Vázquez, Ane Sorraín, José María Marimón Ortiz de Zarate, Ma Dolores Gómez Ruiz, Eva González Barberá, José Luis López Hontangas, José María Navarro-Marí, Irene Pedrosa Corral, Sara Sanbonmatsu Gámez, M. Carmen Perez Gonzalez, Francisco Javier Chamizo López, Ana Bordes Benítez, David Navarro Ortega, Eliseo Albert Vicent, Ignacio Torres, Ma Isabel Gascón Ros, Cristina Torregrosa Hetland, Eva Pastor Boix, Paloma Cascales Ramos, Begoña Fuster Escrivá, Concepción Gimeno Cardona, María Dolores Ocete Mochón, Rafael Medina González, Julia González Cantó, Olalla Martínez Macías, Begoña Palop Borrás, Inmaculada de Toro Peinado, Ma Concepción Mediavilla Gradolph, Mercedes Pérez Ruiz, Oscar González-Recio, Mónica Gutiérrez-Rivas, Encarnación Simarro Córdoba, Julia Lozano Serra, Lorena Robles Fonseca, Adolfo de Salazar, Laura Viñuela, Natalia Chueca, Federico García, Cristina Gomez-Camarasa, Ana Carvajal, Vicente Martín, Juan Fregeneda, Antonio J. Molina, Héctor Arguello, Tania Fernandez-Villa, Amparo Farga Martí, Rocío Falcón, Victoria Domínguez Márquez, José Javier Costa Alcalde, Rocío Trastoy Pena, Gema Barbeito Castiñeiras, Amparo Coira Nieto, María Luisa Pérez del Molino Bernal, Antonio Aguilera, Anna M. Planas, Álex Soriano, Israel Fernández-Cádenas, Jordi Pérez-Tur, Ma Ángeles Marcos Maeso, Carmen Ezpeleta Baquedano, Ana Navascués Ortega, Ana Miqueleiz Zapatero, Manuel Segovia Hernández, Antonio Moreno Docón, Esther Viedma Moreno, Jesús Mingorance, Juan Carlos Galán Montemayor, Iván Sanz Muñoz, Diana Pérez San José, Maria Gil Fortuño, Juan B. Bellido Blasco, Alberto Yagüe Muñoz, Noelia Henández Pérez, Helena Buj Jordá, Óscar Pérez Olaso, Alejandro González Praetorius, Aida Esperanza Ramírez Marinero, Eduardo Padilla León, Alba Vilas Basil, Mireia Canal Aranda, Albert Bernet Sánchez, Alba Bellés Bellés, Eric López González, Iván Prats Sánchez, Mercè García González, Miguel Martínez Lirola, Maripaz Ventero Martín, Carmen Molina Pardines, Nieves Orta Mira, María Navarro Cots, Inmaculada Vidal Catalá, Isabel García Nava, Soledad Illescas Fernández-Bermejo, José Martínez-Alarcón, Marta Torres-Narbona, Cristina Colmenarejo, Lidia García-Agudo, Jorge Alfredo Pérez García, Martín Yago López, María Ángeles Goberna Bravo, Carolina Pla Cortes, Noelia Lozano Rodríguez, Nieves Aparici Valero, Sandra Moreno Marro, Agustín Irazo Tatay, Isabel Mariscal Pieper, Ma Pilar Ramos, Mónica Parra Grande, Bárbara Gómez Alonso, Francisco José Arjona Zaragoza, Amparo Broseta Tamarit, Juan José Badiola Díez, Alicia Otero García, Eloísa Sevilla Romeo, Belén Marín González, Mirta García Martínez, Marina Betancor Caro, Diego Sola Fraca, Sonia Pérez Lázaro, Eva Monleón Moscardó, Marta Monzón Garcés, Cristina Acín Tresaco, Rosa Bolea Bailo, Bernardino Moreno Burgos, Carlos Gulin Blanco, Nora Mariela Martínez Ramírez, Miguel Ángel Jiménez Clavero, Fernando Lázaro-Perona, Manuel Ponce-Alonso, Cristina Juana Torregrosa-Hetland, Alberto Benguría, Jovita Fernández-Pinero, Victoria Simón García, María Eugenia Carrillo Gil, Antonio Alcamí, Gonzalo Llop Furquet, Mirian Fernández-Alonso, Pedro Luis Garcinuño Enríquez, Mario Rodríguez-Dominguez, María Teresa Cabezas Fernández, Laura Martínez-García, Sara Gonzalez-Bodí, Manuel Ángel Rodríguez Maresca, María Pilar Romero-Gómez, Marta Bermejo Bermejo, María Rodríguez-Tejedor, Irene Muñoz-Gallego, Julio García-Rodríguez, Nieves Felisa Martínez Cameo, Javier Temes, Juan Miguel Fregeneda-Grandes, María Dolores Folgueira, Ana Dopazo, Melanie Abreu Di Berardino, Víctor Manuel Fernández Soria, Raúl Recio Martínez, Sergio Callejas, Ricardo Ramos-Ruiz, Amparo Martínez-Ramírez, Jose María González-Alba, María Paz Ventero Martín, Begoña Aguado, Elias Dahdouh, Mercedes Roig Cardells, Salvador Raga Borja, Verónica Saludes, Cristina Casañ, Isabel Escribano Cañadas, and Fernando Simón Soria.

REFERENCES

- Elbe S, Buckland-Merrett G. 2017. Data, disease and diplomacy: GISAID's innovative contribution to global health. *Glob Chall* 1:33–46. <https://doi.org/10.1002/gch2.1018>.
- Hadfield J, Megill C, Bell SM, Huddleston J, Potter B, Callender C, Sagulenko P, Bedford T, Neher RA. 2018. Nextstrain: real-time tracking of pathogen evolution. *Bioinformatics* 34:4121–4123. <https://doi.org/10.1093/bioinformatics/bty407>.
- Lauring AS, Hodcroft EB. 2021. Genetic variants of SARS-CoV-2—what do they mean? *JAMA* 325:529–531. <https://doi.org/10.1001/jama.2020.27124>.
- Volz E, Hill V, McCrone JT, Price A, Jorgensen D, O'Toole Á, Southgate J, Johnson R, Jackson B, Nascimento FF, Rey SM, Nicholls SM, Colquhoun RM, da Silva Filipe A, Shepherd J, Pascall DJ, Shah R, Jesudason N, Li K, Jarrett R, Pacchiarini N, Bull M, Geidelberg L, Siveroni I, Goodfellow I, Loman NJ, Pybus OG, Robertson DL, Thomson EC, Rambaut A, Connor TR, COG-UK Consortium. 2021. Evaluating the effects of SARS-CoV-2 spike mutation D614G on transmissibility and pathogenicity. *Cell* 184:64–75.E11. <https://doi.org/10.1016/j.cell.2020.11.020>.
- Hodcroft EB, Zuber M, Nadeau S, Vaughan TG, Crawford KHD, Althaus CL, Reichmuth ML, Bowen JE, Walls AC, Corti D, Bloom JD, Veester D, Mateo D, Hermandó A, Comas I, González-Candelas F, González-Candelas F, Goig GA, Chiner-Oms Á, Cancino-Muñoz I, López MG, Torres-Puente M, Gomez-Navarro I, Jiménez-Serrano S, Ruiz-Roldán L, Bracho MA, García-González N, Martínez-Priego L, Galán-Vendrell I, Ruiz-Hueso P, De Marco G, Ferrús ML, Carbo-Ramirez S, D'Auria G, Coscollá M, Ruiz-Rodríguez P, Roig-Sena FJ, Sanmartín I, García-Souto D, Pequeno-Valtierra A, Tubio JMC, Rodríguez-Castro J, Rabella N, Navarro F, Miró E, Rodríguez-Iglesias M, Galán-Sánchez F, Rodríguez-Pallares S, de Toro M, Escudero MB, SeqCOVID-SPAIN consortium, et al. 2021. Spread of a SARS-CoV-2 variant through Europe in the summer of 2020. *Nature* 595:707–712. <https://doi.org/10.1038/s41586-021-03677-y>.
- Oude Munnink BB, Sikkema RS, Nieuwenhuijse DF, Molenaar RJ, Munger E, Molenkamp R, van der Spek A, Tolsma P, Rietveld A, Brouwer M, Bouwmeester-Vincken N, Harders F, Hakze-van der Honing R, Wegdam-Blans MCA, Bouwstra RJ, GeurtsvanKessel C, van der Eijk AA, Velkers FC, Smit LAM, Stegeman A, van der Poel WHM, Koopmans MPG. 2021. Transmission of SARS-CoV-2 on mink farms between humans and mink and back to humans. *Science* 371:172–177. <https://doi.org/10.1126/science.abe5901>.
- Welkers MRA, Han AX, Reusken C, Eggink D. 2021. Possible host-adaptation of SARS-CoV-2 due to improved ACE2 receptor binding in mink. *Virus Evol* 7:veaa094. <https://doi.org/10.1093/ve/veaa094>.
- Young BE, Fong SW, Chan YH, Mak TM, Ang LW, Anderson DE, Lee CY, Amrun SN, Lee B, Goh YS, Su YCF, Wei WE, Kalimuddin S, Chai LYA, Pada S, Tan SY, Sun L, Parthasarathy P, Chen YY, Barkham T, Lin RTP, Maurer-Stroh S, Leo YS, Wang LF, Renia L, Lee VJ, Smith GJD, Lye DC, Ng LFP. 2020. Effects of a major deletion in the SARS-CoV-2 genome on the severity of infection and the inflammatory response: an observational cohort study. *Lancet* 396:603–611. [https://doi.org/10.1016/S0140-6736\(20\)31757-8](https://doi.org/10.1016/S0140-6736(20)31757-8).
- Chand M, Hopkins S, Dabrera G, Achison C, Barclay W, Ferguson N, Volz E, Loman N, Rambaut A, Barrett J. 2020. Investigation of novel SARS-CoV-2 variant. Variant of concern 202012/01. https://assets.publishing.service.gov.uk/government/uploads/system/uploads/attachment_data/file/959438/Technical_Briefing_VOC_SH_NJL2_SH2.pdf.
- Walls AC, Park YJ, Tortorici MA, Wall A, McGuire AT, Veester D. 2020. Structure, function, and antigenicity of the SARS-CoV-2 spike glycoprotein. *Cell* 181:281–292.E6. <https://doi.org/10.1016/j.cell.2020.02.058>.
- Salvatori G, Luberto L, Maffei M, Aurisicchio L, Roscilli G, Palombo F, Marra E. 2020. SARS-CoV-2 spike protein: an optimal immunological target for vaccines. *J Transl Med* 18:222. <https://doi.org/10.1186/s12967-020-02392-y>.
- Turoňová B, Sikora M, Schürmann C, Hagen WJH, Welsch S, Blanc FEC, von Bülow S, Gecht M, Bagola K, Hörner C, van Zandbergen G, Landry J, de Azevedo NTD, Mosalaganti S, Schwarz A, Covino R, Mühlebach MD, Hummer G, Krijnse Locker J, Beck M. 2020. In situ structural analysis of SARS-CoV-2 spike reveals flexibility mediated by three hinges. *Science* 370:203–208. <https://doi.org/10.1126/science.abd5223>.
- Hoffmann M, Kleine-Weber H, Pöhlmann S. 2020. A multibasic cleavage site in the spike protein of SARS-CoV-2 is essential for infection of human lung cells. *Mol Cell* 78:779–784.E5. <https://doi.org/10.1016/j.molcel.2020.04.022>.
- Hoffmann M, Kleine-Weber H, Schroeder S, Krüger N, Herrler T, Erichsen S, Schiergens TS, Herrler G, Wu N-H, Nitsche A, Müller MA, Drosten C, Pöhlmann S. 2020. SARS-CoV-2 cell entry depends on ACE2 and TMPRSS2 and is blocked by a clinically proven protease inhibitor. *Cell* 181:271–280.E8. <https://doi.org/10.1016/j.cell.2020.02.052>.
- Kielian M. 2014. Mechanisms of virus membrane fusion proteins. *Annu Rev Virol* 1:171–189. <https://doi.org/10.1146/annurev-virology-031413-085521>.
- Korber B, Fischer WM, Gnanakaran S, Yoon H, Theiler J, Abfalterer W, Hengartner N, Giorgi EE, Bhattacharya T, Foley B, Hastie KM, Parker MD, Partridge DG, Evans CM, Freeman TM, de Silva TI, McDanal C, Perez LG, Tang H, Moon-Walker A, Whelan SP, LaBranche CC, Saphire EO, Montefiori DC, Sheffield COVID-19 Genomics Group. 2020. Tracking changes in SARS-CoV-2 spike: evidence that D614G increases infectivity of the COVID-19 virus. *Cell* 182:812–827.E19. <https://doi.org/10.1016/j.cell.2020.06.043>.
- Hou YJ, Chiba S, Halfmann P, Ehre C, Kuroda M, Dinnon KH, 3rd, Leist SR, Schäfer A, Nakajima N, Takahashi K, Lee RE, Mascenik TM, Graham R, Edwards CE, Tse LV, Okuda K, Markmann AJ, Bartelt L, de Silva A, Margolis DM, Boucher RC, Randell SH, Suzuki T, Gralinski LE, Kawaoka Y, Baric RS. 2020. SARS-CoV-2 D614G variant exhibits efficient replication ex vivo and transmission in vivo. *Science* 370:1464–1468. <https://doi.org/10.1126/science.abe8499>.
- Plante JA, Liu Y, Liu J, Xia H, Johnson BA, Lokugamage KG, Zhang X, Muruato AE, Zou J, Fontes-Garfias CR, Mirchandani D, Scharton D, Billelo JP, Ku Z, An Z, Kalveram B, Freiberg AN, Menachery VD, Xie X, Plante KS, Weaver SC, Shi PY. 2021. Spike mutation D614G alters SARS-CoV-2 fitness. *Nature* 592:116–121. <https://doi.org/10.1038/s41586-020-2895-3>.
- Zhou B, Thi Nhu Thao T, Hoffmann D, Taddeo A, Ebert N, Labroussaa F, Pohlmann A, King J, Steiner S, Kelly JN, Portmann J, Halwe NJ, Ulrich L, Trüeb BS, Fan X, Hoffmann B, Wang L, Thomann L, Lin X, Stalder H, Pozzi B, de Brot S, Jiang N, Cui D, Hossain J, Wilson M, Keller M, Stark TJ, Barnes JR, Dijkman R, Jores J, Benarafa C, Wentworth DE, Thiel V, Beer M. 2021. SARS-CoV-2 spike D614G change enhances replication and transmission. *Nature* 592:122–127. <https://doi.org/10.1038/s41586-021-03361-1>.
- Daniloski Z, Jordan TX, Ilmain JK, Guo X, Bhabha G, tenOever BR, Sanjana NE. 2021. The spike D614G mutation increases SARS-CoV-2 infection of multiple human cell types. *Elife* 10:e65365. <https://doi.org/10.7554/eLife.65365>.
- Larsen HD, Fonager J, Lomholt FK, Dalby T, Benedetti G, Kristensen B, Urth TR, Rasmussen M, Lassaunière R, Rasmussen TB, Strandbygaard B, Lohse L, Chaine M, Møller KL, Berthelsen AN, Nørgaard SK, Sönksen UW, Boklund AE, Hammer AS, Belsham GJ, Krause TG, Mortensen S, Bøtner A, Fomsgaard A, Mølbak K. 2021. Preliminary report of an outbreak of SARS-CoV-2 in mink and mink farmers associated with community spread, Denmark, June to November 2020. *Euro Surveill* 26:210009. <https://doi.org/10.2807/1560-7917.ES.2021.26.5.210009>.
- Rodrigues J, Barrera-Vilarmas S, J MCT, Sorokina M, Seckel E, Kastriitis PL, Levitt M. 2020. Insights on cross-species transmission of SARS-CoV-2 from structural modeling. *PLoS Comput Biol* 16:e1008449. <https://doi.org/10.1371/journal.pcbi.1008449>.
- WHO. 2021. Tracking SARS-CoV-2 variants. <https://www.who.int/en/activities/tracking-SARS-CoV-2-variants/>. Accessed 1 August 2021.
- Public Health England. 2021. SARS-CoV-2 variants of concern and variants under investigation in England. Technical briefing 19.
- Leung K, Shum MH, Leung GM, Lam TT, Wu JT. 2021. Early transmissibility assessment of the N501Y mutant strains of SARS-CoV-2 in the United Kingdom, October to November 2020. *Euro Surveill* 26:2002106. <https://doi.org/10.2807/1560-7917.ES.2020.26.1.2002106>.
- Galloway S, Paul P, MacCannell D, Johansson M, Brooks J, MacNeil A, Slayton R, Tong S, Silk B, Armstrong G, Biggerstaff M, Dugan V. 2021. Emergence of SARS-CoV-2 B.1.1.7 lineage—United States, December 29, 2020–January 12, MMWR Morbid Mortal Wkly Rep 70:95–99. <https://doi.org/10.15585/mmwr.mm7003e2>.
- Davies NG, Abbott S, Barnard RC, Jarvis CI, Kucharski AJ, Munday JD, Pearson CAB, Russell TW, Tully DC, Washburne AD, Wenseleers T, Gimma A, Waites W, Wong KLM, van Zandvoort K, Silverman JD, Diaz-Ordaz K, Keogh R, Eggo RM, Funk S, Jit M, Atkins KE, Edmunds WJ, CMMID COVID-19 Working Group. 2021. Estimated transmissibility and impact of SARS-CoV-2 lineage B.1.1.7 in England. *Science* 372:eabg3055. <https://doi.org/10.1126/science.abg3055>.
- Lucas C, Vogels CBF, Yildirim I, Rothman JE, Lu P, Monteiro V, Gelhausen JR, Campbell M, Silva J, Tabachikova A, Muenker MC, Breban MI, Fauver JR, Mohanty S, Huang J, Initiative Y-C-G, Pearson C, Muyombwe A, Downing R, Razeq J, Petrone M, Ott I, Watkins A, Kalinich C, Alpert T, Brito A, Earnest R, Murphy S, Neal C, Laszlo E, Altajar A, Tikhonova I, Castaldi C, Mane S, Bilguvar K, Kerantzas N, Ferguson D, Schulz W, Landry M, Peaper D, Shaw AC, Ko AI, Omer SB, Grubaugh ND, Iwasaki A. 11 October 2021. Impact of circulating SARS-CoV-2 variants on mRNA vaccine-induced immunity. *Nature* <https://doi.org/10.1038/s41586-021-04085-y>.

29. Lopez Bernal J, Andrews N, Gower C, Gallagher E, Simmons R, Thelwall S, Stowe J, Tessier E, Groves N, Dabrera G, Myers R, Campbell CNJ, Amirthalingam G, Edmunds M, Zambon M, Brown KE, Hopkins S, Chand M, Ramsay M. 2021. Effectiveness of Covid-19 vaccines against the B.1.617.2 (delta) variant. *N Engl J Med* 385:585–594. <https://doi.org/10.1056/NEJMoa2108891>.
30. López MG, Chiner-Oms Á, de Viedma DG, Ruiz-Rodríguez P, Bracho MA, Cancino-Muñoz I, D'Auria G, de Marco G, García-González N, Goig GA, Gómez-Navarro I, Jiménez-Serrano S, Martínez-Priego L, Ruiz-Hueso P, Ruiz-Roldán L, Torres-Puente M, Alberola J, Albert E, Zaldumbide MA, Bea-Escudero MP, Boga JA, Bordoy AE, Canut-Blasco A, Carvajal A, Eguiluz GC, Rodríguez MLC, Costa-Alcalde JJ, de Toro M, de Toro Peinado I, del Pozo JL, Duchêne S, Fernández-Pinero J, Escrivá BF, Cardona CG, Galán VG, Jiménez NG, Crespo SH, Herranz M, Lepe JA, López-Hontangas JL, Marcos MÁ, Martín V, Martró E, Beamonte AM, Ros MM, Moreno-Muñoz R, Navarro D, Navarro-Marí JM, Not A, Oliver A, et al. 30 September 2021. The first wave of the COVID-19 epidemic in Spain was associated with early introductions and fast spread of a dominating genetic variant. *Nat Genet* 53:1405–1414. <https://doi.org/10.1038/s41588-021-00936-6>.
31. Washington NL, Gangavarapu K, Zeller M, Bolze A, Cirulli ET, Barrett KMS, Larsen BB, Anderson C, White S, Cassens T, Jacobs S, Levan G, Nguyen J, Ramirez JM, Rivera-García C, Sandoval E, Wang X, Wong D, Spencer E, Robles-Sikisaka R, Kurzban E, Hughes LD, Deng X, Wang C, Servellita V, Valentine H, De Hoff P, Seaver P, Sathe S, Gietzen K, Sickler B, Antico J, Hoon K, Liu J, Harding A, Bakhtar O, Basler T, Austin B, Isaksson M, Febbo PG, Becker D, Laurent M, McDonald E, Yeo GW, Knight R, Laurent LC, de Feo E, Worobey M, Chiu C, Suchard MA, et al. 30 March 2021. Emergence and rapid transmission of SARS-CoV-2 B.1.1.7 in the United States. *Cell* 184(10):2587–2594.E7. <https://doi.org/10.1016/j.cell.2021.03.052>.
32. Tegally H, Wilkinson E, Giovanetti M, Iranzadeh A, Fonseca V, Giandhari J, Doolabh D, Pillay S, San EJ, Msomi N, Mlisana K, von Gottberg A, Walaza S, Allam M, Ismail A, Mohale T, Glass AJ, Engelbrecht S, Van Zyl G, Praies V, Petruccione F, Sigal A, Hardie D, Marais G, Hsiao M, Korsman S, Davier M-A, Tyers L, Mudau I, York D, Maslo C, Goedhals D, Abrahams S, Laguda-Akingba O, Alisoltani-Dehkordi A, Godzik A, Wibmer CK, Sewell BT, Lourenço J, Alcantara LCJ, Pond SLK, Weaver S, Martin D, Lessells RJ, Bhiman JN, Williamson C, de Oliveira T. 9 March 2021. Detection of a SARS-CoV-2 variant of concern in South Africa. *Nature* 592:438–443. <https://doi.org/10.1038/s41586-021-03402-9>.
33. Rambaut A, Holmes EC, O'Toole Á, Hill V, McCrone JT, Ruis C, Du Plessis L, Pybus OG. 2020. A dynamic nomenclature proposal for SARS-CoV-2 lineages to assist genomic epidemiology. *Nat Microbiol* 5:1403–1407. <https://doi.org/10.1038/s41564-020-0770-5>.
34. Reference deleted.
35. Hodcroft EB. 2021. CoVariants: SARS-CoV-2 mutations and variants of interest. <https://covariants.org/>. Accessed 1 August 2021.
36. Nelson G, Buzko O, Spilman P, Niazi K, Rabizadeh S, Soon-Shiong P. 2021. Molecular dynamic simulation reveals E484K mutation enhances spike RBD-ACE2 affinity and the combination of E484K, K417N and N501Y mutations (501Y.V2 variant) induces conformational change greater than N501Y mutant alone, potentially resulting in an escape mutant. *bioRxiv* <https://doi.org/10.1101/2021.01.13.426558>;2021.01.13.426558.
37. Liu Z, VanBlargan LA, Bloyet L-M, Rothlauf PW, Chen RE, Stumpf S, Zhao H, Errico JM, Theel ES, Liebeskind MJ, Alford B, Buchser WJ, Ellebedy AH, Fremont DH, Diamond MS, Whelan SPJ. 2021. Landscape analysis of escape variants identifies SARS-CoV-2 spike mutations that attenuate monoclonal and serum antibody neutralization. *bioRxiv* <https://doi.org/10.1101/2020.11.06.372037>;2020.11.06.372037.
38. McCallum M, Marco AD, Lempp F, Tortorici MA, Pinto D, Walls AC, Beltramello M, Chen A, Liu Z, Zatta F, Zepeda S, di Iulio J, Bowen JE, Montiel-Ruiz M, Zhou J, Rosen LE, Bianchi S, Guarino B, Fregni CS, Abdelnabi R, Caroline Foo S-Y, Rothlauf PW, Bloyet L-M, Benigni F, Camerani E, Neyts J, Riva A, Snell G, Telenti A, Whelan SPJ, Virgin HW, Corti D, Pizzuto MS, Veeler D. 16 March 2021. N-terminal domain antigenic mapping reveals a site of vulnerability for SARS-CoV-2. *Cell* 184(9):2332–2347.E16. <https://doi.org/10.1016/j.cell.2021.03.028>.
39. Huang Y, Yang C, Xu X-F, Xu W, Liu S-W. 2020. Structural and functional properties of SARS-CoV-2 spike protein: potential antiviral drug development for COVID-19. *Acta Pharmacol Sin* 41:1141–1149. <https://doi.org/10.1038/s41401-020-0485-4>.
40. Xia S, Zhu Y, Liu M, Lan Q, Xu W, Wu Y, Ying T, Liu S, Shi Z, Jiang S, Lu L. 2020. Fusion mechanism of 2019-nCoV and fusion inhibitors targeting HR1 domain in spike protein. *Cell Mol Immunol* 17:765–767. <https://doi.org/10.1038/s41423-020-0374-2>.
41. Lu R, Zhao X, Li J, Niu P, Yang B, Wu H, Wang W, Song H, Huang B, Zhu N, Bi Y, Ma X, Zhan F, Wang L, Hu T, Zhou H, Hu Z, Zhou W, Zhao L, Chen J, Meng Y, Wang J, Lin Y, Yuan J, Xie Z, Ma J, Liu WJ, Wang D, Xu W, Holmes EC, Gao GF, Wu G, Chen W, Shi W, Tan W. 2020. Genomic characterisation and epidemiology of 2019 novel coronavirus: implications for virus origins and receptor binding. *Lancet* 395:565–574. [https://doi.org/10.1016/S0140-6736\(20\)30251-8](https://doi.org/10.1016/S0140-6736(20)30251-8).
42. Xia S, Xu W, Wang Q, Wang C, Hua C, Li W, Lu L, Jiang S. 2018. Peptide-based membrane fusion inhibitors targeting HCoV-229E spike protein HR1 and HR2 domains. *Int J Mol Sci* 19:487. <https://doi.org/10.3390/ijms19020487>.
43. Cai Y, Zhang J, Xiao T, Peng H, Sterling SM, Walsh RM, Rawson S, Rits-Volloch S, Chen B. 2020. Distinct conformational states of SARS-CoV-2 spike protein. *Science* 369:1586–1592. <https://doi.org/10.1126/science.abd4251>.
44. Fan X, Cao D, Kong L, Zhang X. 2020. Cryo-EM analysis of the post-fusion structure of the SARS-CoV spike glycoprotein. *Nat Commun* 11:3618. <https://doi.org/10.1038/s41467-020-17371-6>.
45. Zhang L, Jackson CB, Mou H, Ojha A, Peng H, Quinlan BD, Rangarajan ES, Pan A, Vanderheiden A, Suthar MS, Li W, Izard T, Rader C, Farzan M, Choe H. 2020. SARS-CoV-2 spike-protein D614G mutation increases virion spike density and infectivity. *Nat Commun* 11:6013. <https://doi.org/10.1038/s41467-020-19808-4>.
46. Yurkovetskiy L, Wang X, Pascal KE, Tomkins-Tinch C, Nyalile TP, Wang Y, Baum A, Diehl WE, Dauphin A, Carbone C, Veinotte K, Egri SB, Schaffner SF, Lemieux JE, Munro JB, Rafique A, Barve A, Sabeti PC, Kyrtatsous CA, Dudkina NV, Shen K, Luban J. 2020. Structural and functional analysis of the D614G SARS-CoV-2 spike protein variant. *Cell* 183:739–751.E8. <https://doi.org/10.1016/j.cell.2020.09.032>.
47. Wang Y, Wu J, Zhang L, Zhang Y, Wang H, Ding R, Nie J, Li Q, Liu S, Yu Y, Yang X-M, Qu X, Duan K, Huang W. 2021. The infectivity and antigenicity of epidemic SARS-CoV-2 variants in the United Kingdom. *Res Square* <https://doi.org/10.21203/rs.3.rs-153108/v1>.
48. Berger Rentsch M, Zimmer G. 2011. A vesicular stomatitis virus replicon-based bioassay for the rapid and sensitive determination of multi-species type I interferon. *PLoS One* 6:e25858. <https://doi.org/10.1371/journal.pone.0025858>.
49. Weissman D, Alameh M-G, de Silva T, Collini P, Hornsby H, Brown R, LaBranche CC, Edwards RJ, Sutherland L, Santra S, Mansouri K, Gobeil S, McDanal C, Pardi N, Hengartner N, Lin PJC, Tam Y, Shaw PA, Lewis MG, Boesler C, Şahin U, Acharya P, Haynes BF, Korber B, Montefiori DC. 2021. D614G spike mutation increases SARS CoV-2 susceptibility to neutralization. *Cell Host Microbe* 29:23–31.E4. <https://doi.org/10.1016/j.chom.2020.11.012>.
50. Li Y, Lai D-y, Zhang H-n, Jiang H-w, Tian X, Ma M-l, Qi H, Meng Q-f, Guo S-j, Wu Y, Wang W, Yang X, Shi D-w, Dai J-b, Ying T, Zhou J, Tao S-c. 2020. Linear epitopes of SARS-CoV-2 spike protein elicit neutralizing antibodies in COVID-19 patients. *Cell Mol Immunol* 17:1095–1097. <https://doi.org/10.1038/s41423-020-00523-5>.
51. Mateus J, Grifoni A, Tarke A, Sidney J, Ramirez SI, Dan JM, Burger ZC, Rawlins SA, Smith DM, Phillips E, Mallal S, Lammers M, Rubiro P, Quiambao L, Sutherland A, Yu ED, da Silva Antunes R, Greenbaum J, Frazier A, Markmann AJ, Premkumar L, de Silva A, Peters B, Crotty S, Sette A, Weiskopf D. 2020. Selective and cross-reactive SARS-CoV-2 T cell epitopes in unexposed humans. *Science* 370:89–94. <https://doi.org/10.1126/science.abd3871>.
52. Yi Z, Ling Y, Zhang X, Chen J, Hu K, Wang Y, Song W, Ying T, Zhang R, Lu H, Yuan Z. 2020. Functional mapping of B-cell linear epitopes of SARS-CoV-2 in COVID-19 convalescent population. *Emerg Microbes Infect* 9:1988–1996. <https://doi.org/10.1080/22221751.2020.1815591>.
53. Wang Z, Schmidt F, Weisblum Y, Muecksch F, Barnes CO, Finkin S, Schaefer-Babajew D, Cipolla M, Gaebler C, Lieberman JA, Oliveira TY, Yang Z, Abernathy ME, Huey-Tubman KE, Hurley A, Turroja M, West KA, Gordon K, Millard KG, Ramos V, Silva JD, Xu J, Colbert RA, Patel R, Dizon J, Unson-O'Brien C, Shimeliovich I, Gazumyan A, Caskey M, Bjorkman PJ, Casellas R, Hatzioannou T, Bieniasz PD, Nussenzweig MC. 2021. mRNA vaccine-elicited antibodies to SARS-CoV-2 and circulating variants. *Nature* 592:616–622. <https://doi.org/10.1038/s41586-021-03324-6>.
54. Wibmer CK, Ayres F, Hermandus T, Madzivhandila M, Kgagudi P, Lambson BE, Vermeulen M, van den Berg K, Rossouw T, Boswell M, Ueckermann V, Meiring S, von Gottberg A, Cohen C, Morris L, Bhiman JN, Moore PL. 2 March 2021. SARS-CoV-2 501Y.V2 escapes neutralization by South African COVID-19 donor plasma. *Nat Med* 27:622–625. <https://doi.org/10.1038/s41591-021-01285-x>.
55. Zhao J, Zhao S, Ou J, Zhang J, Lan W, Guan W, Wu X, Yan Y, Zhao W, Wu J, Chodosh J, Zhang Q. 2020. COVID-19: coronavirus vaccine development

- updates. *Front Immunol* 11:602256. <https://doi.org/10.3389/fimmu.2020.602256>.
56. Izda V, Jeffries MA, Sawalha AH. 2021. COVID-19: a review of therapeutic strategies and vaccine candidates. *Clin Immunol* 222:108634. <https://doi.org/10.1016/j.clim.2020.108634>.
 57. Pond S. Natural selection analysis of global SARS-CoV-2/COVID-19 enabled by data from GISAID. <https://observablehq.com/@spond/revised-sars-cov-2-analytics-page?collection=@spond/sars-cov-2>. Accessed 19 February 2021.
 58. Grubaugh ND, Gangavarapu K, Quick J, Matteson NL, De Jesus JG, Main BJ, Tan AL, Paul LM, Brackney DE, Grewal S, Gurfield N, Van Rompay KKA, Isern S, Michael SF, Coffey LL, Loman NJ, Andersen KG. 2019. An amplicon-based sequencing framework for accurately measuring intrahost virus diversity using PrimalSeq and iVar. *Genome Biol* 20:8. <https://doi.org/10.1186/s13059-018-1618-7>.
 59. Wood DE, Salzberg SL. 2014. Kraken: ultrafast metagenomic sequence classification using exact alignments. *Genome Biol* 15:R46. <https://doi.org/10.1186/gb-2014-15-3-r46>.
 60. Quick J. 2020. nCoV-2019 sequencing protocol. <https://www.protocols.io/view/ncov-2019-sequencing-protocol-v3-locost-bh42j8ye>. Accessed 1 August 2021.
 61. Artic Network. 2020. Artic-network/artic-ncov2019. <https://github.com/artic-network/artic-ncov2019>. Accessed 1 August 2021.
 62. Chen S, Zhou Y, Chen Y, Gu J. 2018. fastp: an ultra-fast all-in-one FASTQ pre-processor. *Bioinformatics* 34:i884–i890. <https://doi.org/10.1093/bioinformatics/bty560>.
 63. Ewels P, Magnusson M, Lundin S, Käller M. 2016. MultiQC: summarize analysis results for multiple tools and samples in a single report. *Bioinformatics* 32:3047–3048. <https://doi.org/10.1093/bioinformatics/btw354>.
 64. Kumar S, Stecher G, Li M, Knyaz C, Tamura K. 2018. MEGA X: Molecular Evolutionary Genetics Analysis across computing platforms. *Mol Biol Evol* 35:1547–1549. <https://doi.org/10.1093/molbev/msy096>.
 65. Wu F, Zhao S, Yu B, Chen Y-M, Wang W, Song Z-G, Hu Y, Tao Z-W, Tian J-H, Pei Y-Y, Yuan M-L, Zhang Y-L, Dai F-H, Liu Y, Wang Q-M, Zheng J-J, Xu L, Holmes EC, Zhang Y-Z. 2020. A new coronavirus associated with human respiratory disease in China. *Nature* 579:265–269. <https://doi.org/10.1038/s41586-020-2008-3>.
 66. Katoh K, Misawa K, Kuma K, Miyata T. 2002. MAFFT: a novel method for rapid multiple sequence alignment based on fast Fourier transform. *Nucleic Acids Res* 30:3059–3066. <https://doi.org/10.1093/nar/gkf436>.
 67. Page AJ, Taylor B, Delaney AJ, Soares J, Seemann T, Keane JA, Harris SR. 2016. SNP-sites: rapid efficient extraction of SNPs from multi-FASTA alignments. *Microb Genom* 2:e000056. <https://doi.org/10.1099/mgen.0.000056>.
 68. Cingolani P, Platts A, Wang LL, Coon M, Nguyen T, Wang L, Land SJ, Lu X, Ruden DM. 2012. A program for annotating and predicting the effects of single nucleotide polymorphisms, SnpEff: SNPs in the genome of *Drosophila melanogaster* strain w1118; iso-2; iso-3. *Fly (Austin)* 6:80–92. <https://doi.org/10.4161/fly.19695>.
 69. Gu Z, Gu L, Eils R, Schlesner M, Brors B. 2014. circlize implements and enhances circular visualization in R. *Bioinformatics* 30:2811–2812. <https://doi.org/10.1093/bioinformatics/btu393>.
 70. Lanfear R. 24 November 2020. A global phylogeny of SARS-CoV-2 sequences from GISAID. Zenodo <https://doi.org/10.5281/zenodo.3958883>.
 71. Nguyen LT, Schmidt HA, von Haeseler A, Minh BQ. 2015. IQ-TREE: a fast and effective stochastic algorithm for estimating maximum-likelihood phylogenies. *Mol Biol Evol* 32:268–274. <https://doi.org/10.1093/molbev/msu300>.
 72. Letunic I, Bork P. 2019. Interactive Tree Of Life (iTOL) v4: recent updates and new developments. *Nucleic Acids Res* 47:W256–W259. <https://doi.org/10.1093/nar/gkz239>.
 73. Wang LG, Lam TT, Xu S, Dai Z, Zhou L, Feng T, Guo P, Dunn CW, Jones BR, Bradley T, Zhu H, Guan Y, Jiang Y, Yu G. 2020. Treeio: an R package for phylogenetic tree input and output with richly annotated and associated data. *Mol Biol Evol* 37:599–603. <https://doi.org/10.1093/molbev/msz240>.
 74. Xia S, Liu M, Wang C, Xu W, Lan Q, Feng S, Qi F, Bao L, Du L, Liu S, Qin C, Sun F, Shi Z, Zhu Y, Jiang S, Lu L. 2020. Inhibition of SARS-CoV-2 (previously 2019-nCoV) infection by a highly potent pan-coronavirus fusion inhibitor targeting its spike protein that harbors a high capacity to mediate membrane fusion. *Cell Res* 30:343–355. <https://doi.org/10.1038/s41422-020-0305-x>.
 75. Emsley P, Lohkamp B, Scott WG, Cowtan K. 2010. Features and development of Coot. *Acta Crystallogr D Biol Crystallogr* 66:486–501. <https://doi.org/10.1107/S0907444910007493>.
 76. Gozalbo-Rovira R, Gimenez E, Latorre V, Francés-Gómez C, Albert E, Buesa J, Marina A, Blasco ML, Signes-Costa J, Rodríguez-Díaz J, Geller R, Navarro D. 2020. SARS-CoV-2 antibodies, serum inflammatory biomarkers and clinical severity of hospitalized COVID-19 patients. *J Clin Virol* 131:104611. <https://doi.org/10.1016/j.jcv.2020.104611>.
 77. Woo H, Park S-J, Choi YK, Park T, Tanveer M, Cao Y, Kern NR, Lee J, Yeom MS, Croll TI, Seok C, Im W. 2020. Developing a fully glycosylated full-length SARS-CoV-2 spike protein model in a viral membrane. *J Phys Chem B* 124: 7128–7137. <https://doi.org/10.1021/acs.jpcc.0c04553>.